ABSTRACT

SHOGREN, TYLER JAMES. Cycloparaphenylene Metal Complexes and Variable Macrocyclization; and New Chromium Carbonyl Coupling Reaction. (Under the direction of Walter Weare.)

This thesis describes two different research projects: work done with cycloparaphenylene and the discovery of a new carbon-carbon coupling reaction with metal carbonyls. The first chapter describes the synthesis of the first metal complexes with cycloparaphenylene and the modification of the synthesis of cycloparaphenylene to produce variable sized molecular hoops. The second chapter describes the discovery of a new carbon-carbon coupling reaction using chromium carbonyl that appears similar in some respects to the McMurry reaction.

Cycloparaphenylene Metal Complexes and Variable Macrocyclization; and New Chromium Carbonyl Coupling Reaction

by
Tyler James Shogren

A thesis submitted to the Graduate Faculty of
North Carolina State University
in partial fulfillment of the
requirements for the degree of
Master of Science

Chemistry

Raleigh, North Carolina

2014

APPROVED BY:

_____	_____
Walter Weare Committee Chair	Reza Ghiladi
_____	
Stefan Franzen	

BIOGRAPHY

Tyler Shogren grew up in a small Wisconsin town. He attended UW – Madison, earning a Bachelors of Arts degree in English, before attending UW – Stevens Point, earning a Bachelors of Science degree in Chemistry. At UW – Stevens Point he participated in undergraduate research, studying the sharpening of carbon fiber under corona discharge plasma and also fabricated nanodimensional diamond electrodes for the deposition of nanowires. His work at NCSU is inspired by a passion for nanochemistry.

ACKNOWLEDGMENTS

I'd like to thank Walter Weare for excellent advice throughout my degree. I'd also like to thank the Shultz and Gorman groups for their support and helpful discussion.

TABLE OF CONTENTS

LIST OF FIGURES

LIST OF SCHEMES

LIST OF TABLES

CHAPTER 1

Abstract. This chapter motivates work with cycloparaphenylene, a fascinating allotrope of carbon. The literature and current theory of cycloparaphenylene are reviewed. Modification of one synthesis of cycloparaphenylene to produce a wider variety of hoops sizes is described. Three sizes of cycloparaphenylene are metallated with chromium carbonyl and the trends of the IR C-O stretching peaks are discussed in relation to published electrochemical data.

Introduction. Computer technology continues to alter human society in fundamental ways. Google and the internet make what you know less important than what you can search for[1]. For over half a century advances in photolithography have produced generation after generation of smaller, faster and cheaper computer technology[2] integrated more and more seamlessly with society. Extrapolation of this trend leads one to imagine fantastic future technologies, but this trend must end for fundamental reasons[3,4,5].

Molecular electronics[6] is one of a number of fields growing to replace photolithography[7]. Carbon nanotubes[8] and graphene (Figure 1) have received a lot of

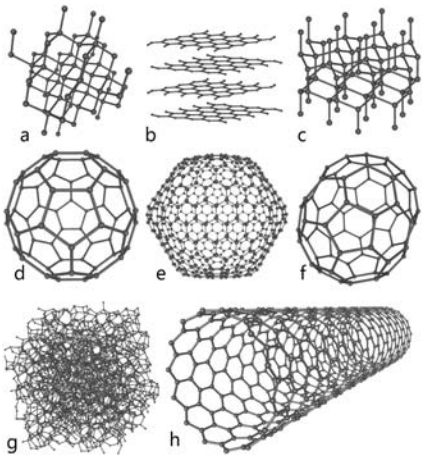

Figure 1. Carbon Allotropes; a) diamond, b) graphite, c) lonsdaleite, d) C_{60}, e) C_{540}, f) C_{70}, g) amorphous carbon, and h) single-walled carbon nanotube. Image from Wikipedia.

attention based on their electronic and thermal conductivities as well as their tunable band gaps. Atomic control of these materials could produce the smallest electronic devices possible. However, much is required before considering these possibilities.

Carbon nanotubes grown on catalytic nanoparticles generate a forest of random tubes. This mixture is random both in chirality, which dictates bandgap[9], and diameter, which makes purification of one type difficult and still unperfected[10]. Once a single type can be isolated, it needs to be arranged with other molecules to form a functional device. This would be difficult even without considering the low solubility of nanotubes. If carbon nanotubes are a bottom-up solution for advanced electronics, a bottom-up solution for making and manipulating nanotubes should be considered.

Cycloparaphenylene (Figure 2) is the shortest repeat unit of metallic carbon

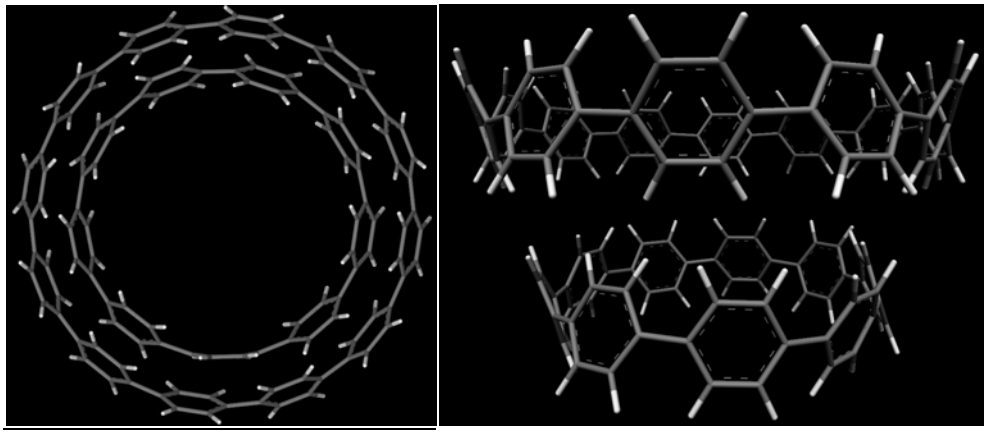

Figure 2. [9]cycloparaphenylene and [12]cycloparaphenylene.

nanotubes[11]. Nanotubes of this type have no bandgap and conduct electricity at least as well as metals. The recent synthesis of cycloparaphenylene represents an opportunity to explore

bottom-up nanotube synthesis as well as add other functional structures that may be useful. Once produced, these additional features might be used to arrange the nanotubes into a device[12].

Covalent functionalization of a nanotube disrupts the aromatic conjugation responsible for the tube's desired electronic properties, so the most successful efforts have involved sidewall decoration[12]. A highly coordinated metal atom bonded to a single hexyl unit of the nanotube should provide a means of self-assembly and a labile molecular contact. Hampered by preferential interactions with solvating functionalities, such a bond has never been demonstrated between a nanotube and a metal atom[13] (Figure 3). Cycloparaphenylene offers the opportunity to explore formation of a metal bond to a strained carbon allotrope with many six-member rings (Figure 4).

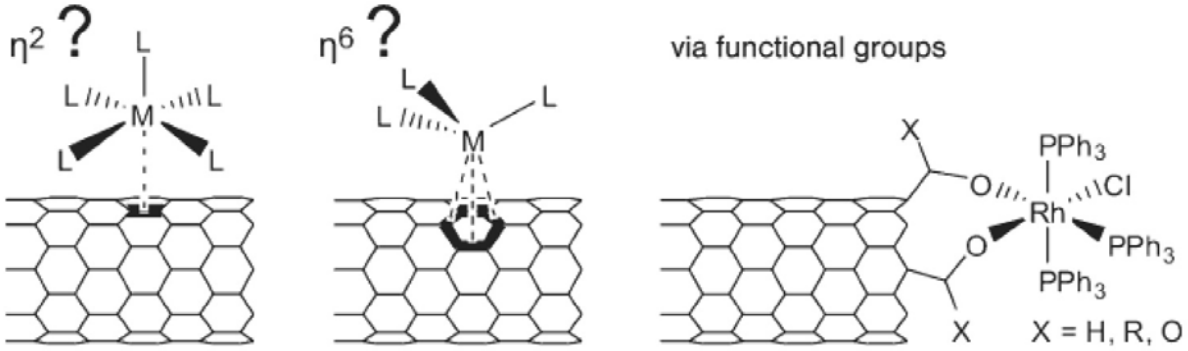

Figure 3. Bonding modes of metal atoms to carbon nanotubes. Metal atoms have not been observed bonding directly to a nanotube sidewall[13].

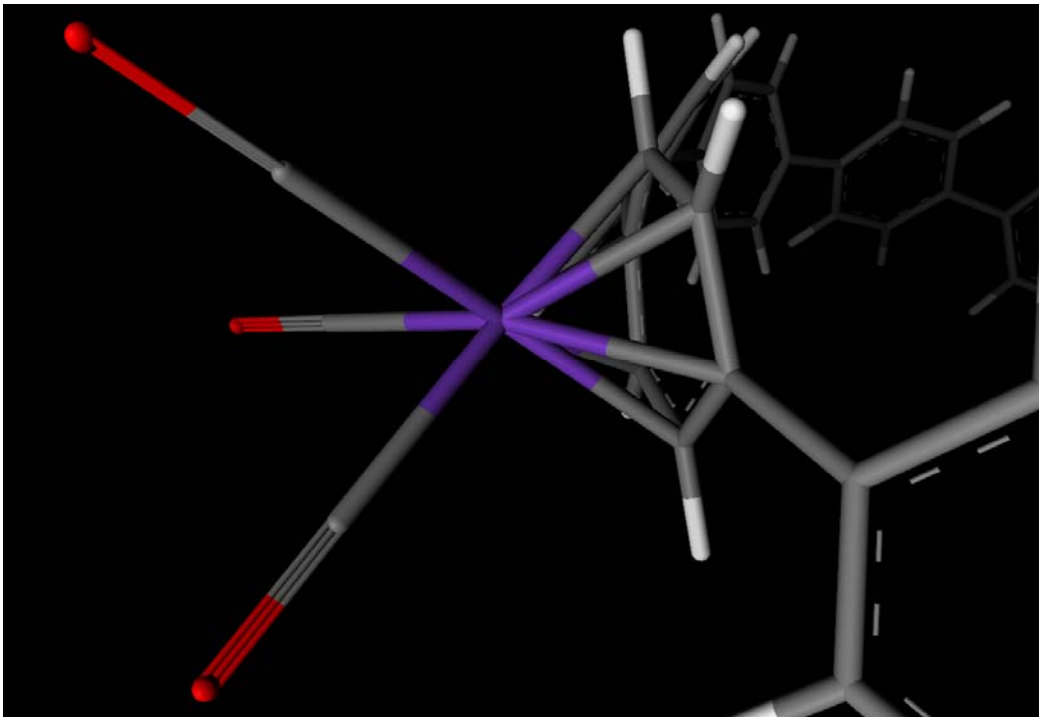

Figure 4. An artist's rendering of a chromium carbonyl complex with cycloparaphenylene.

Literature Review.

Synthesis of Cycloparaphenylene

The first attempt to synthesize cycloparaphenylene was published in 1934[14]. In 1993, Vögtle proposed a series of plausible schemes[15]. It wasn't until recently that researchers discovered a route to this molecule, two of which appear to be based on Vögtle's proposals.

The synthesis of cycloparaphenylene has been achieved by three generally different routes (Figure 5) from three different research groups: Jasti/Bertozzi, Itami and Yamago. The

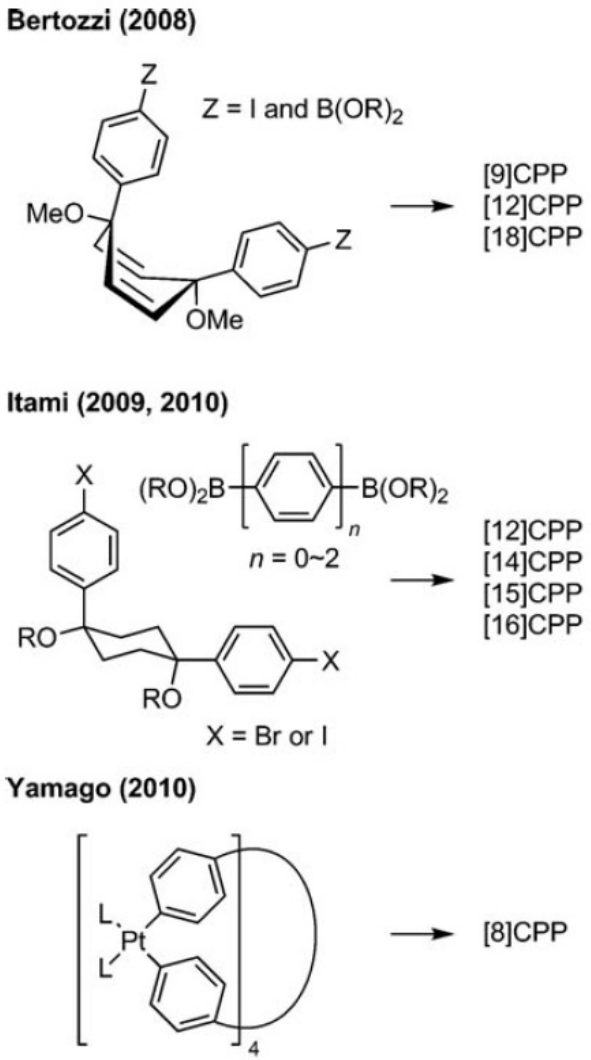

Figure 5. Representative starting units for the synthetic routes to cycloparaphenylene[16].

Jasti/Bertozzi route[17] was published first, in 2008, and was followed by Itami's route[18] in 2009 and Yamago's route[19] in 2010. Following these initial reports, each group has published numerous papers modifying and expanding the utility of their particular route.

Jasti and Bertozzi published the first successful synthesis of cycloparaphenylene relying on a "masked" benzene in the form of 1,4-cyclohexadiene units to form an intermediate macrocycle with strain attenuated by sp^3 carbons (Figure 5). The coupling is

uncontrolled and relies on the termini of intermediate oligomers being coupled together to complete the macrocycle. This coupling reaction produced macrocycles that, once aromatized by sodium naphthalenide, corresponded to [9]-, [12]- and [18]cycloparaphenylene.

Itami's 2009 publication employs a similar strategy, masking with cyclohexane-diols instead of cyclohexadiene (Figure 5). In this case, however, the initial coupling of the iodo/boronic trimers produce a trimer-of-trimers (containing six phenyl and three cyclohexyl substituents) and is completed by subsequent coupling of a fourth trimer. To oxidize the cyclohexyl-diol units, the macrocycle is heated under acidic conditions in a microwave, dehydrating to cyclohexadienyl and aromatizing to phenyl in one pot. Unfortunately, they did not speculate on the mechanism of this final reaction or describe failed reaction conditions.

The third route to cycloparaphenylene is a significant departure from the first two. Yamago, et. al. form an organometallic square composed of four platinum "corners" with covalently bonded biphenyl sides. Subsequent addition of bromide induces reductive elimination, coupling the biphenyl subunits at the para position and forming [8]cycloparaphenylene.

Following these initial reports, Jasti has revised his strategy, making it stepwise (rather than the uncontrolled coupling first reported), and produced [7]cycloparaphenylene[20] and then [6]cycloparaphenylene[21], the smallest currently reported. They have one report of a substituted cycloparaphenylene, incorporating a tetraphenyl-substituted phenyl within [12]cycloparaphenylene[22]. Most recently, they have elucidated selective synthesis of [7]-[12]cycloparaphenylene[23] and published gram-scale syntheses of [8]- and [10]cycloparaphenylene using their same general methods[24]. This last marks the first gram scale synthesis of this class of molecules.

Experimental Evidence of Fundamental Properties

Following their synthesis, the fundamental properties of cycloparaphenylenes have been explored by experiment. These include electronic absorption spectroscopy, electrochemistry, NMR and X-ray crystallography. The results of these experiments underscore the unique electronic and physical properties of cpps.

In their initial synthetic publication, Jasti and Bertozzi reported the interesting electronic excitation and fluorescence spectra of [9]-, [12]- and [18]cycloparaphenylene[17] (Figure 6). They observed the size-independent absorption maximum at ~340 nm and large,

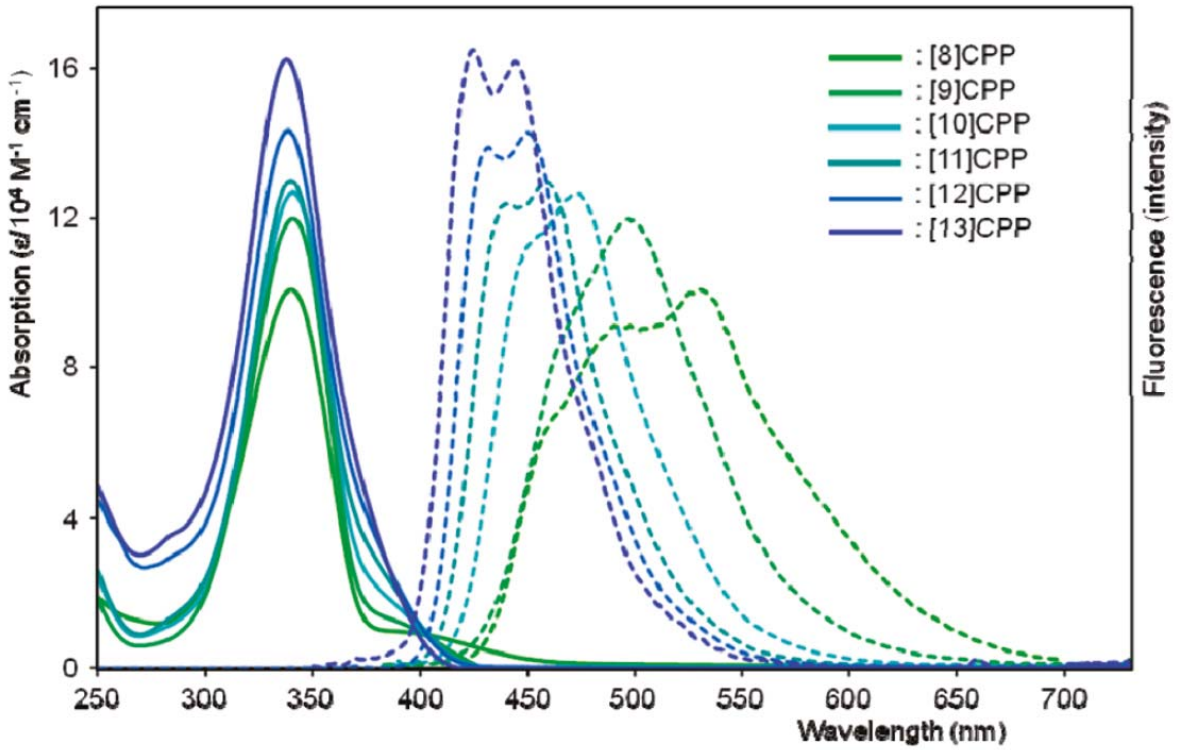

Figure 6. Absorption and fluorescence spectra of [8]-[13]cycloparaphenylene[25].

size dependent Stokes shift. Yamago confirmed these results with their synthesis of [8]cycloparaphenylene and reported the first absorption coefficient ($\varepsilon = 34200\ M^{-1}cm^{-1}$)[19].

In Yamago's follow-up publication describing random and selective synthesis of [8]-[13]cycloparaphenylenes they report the absorbance and fluorescence spectra for all those sizes (Figure 6), showing results consistent with the trends previously observed and noting for the first time that the fluorescence spectra are composed of at least two components[25]. Jasti, et. al. again reported the UV-Vis and fluorescence spectra with their synthesis of [7]cycloparaphenylene[20] and [6]cpp[21]. While [7]cycloparaphenylene is generally consistent with the features and trends of the larger sizes, [6]cpp is reported to have no fluorescence. With these observations, both Yamago and Jasti offer theoretical explanations based on computational results that will be discussed in the following section.

Yamago reports the first electrochemical experiments on cycloparaphenylene[25]. Conducting cyclic voltammetry on [8]-[13]cycloparaphenylene, they demonstrate the redox potential is size dependent, the half-wave potentials ranging from 0.59 V for [8]cpp to 0.85 V for [13]cpp. A similar CV of [6]cycloparaphenylene is reported by Jasti with his synthesis of that molecule[21]. [6]cycloparaphenylene has an oxidation half-wave potential of 0.44 V, consistent with the trend reported by Yamago. Both groups explicitly report no observed reduction waves within the solvent window.

In all cases, NMR experiments have shown the protons and the two types of carbons within any given cycloparaphenylene to be equivalent. These results are interesting because computational studies repeatedly demonstrate energy minimum conformations with certain dihedral angles for different sizes of cycloparaphenylene. The NMR results indicate that free rotation between phenyl units is the general case at room temperature on the NMR timescale. The proton chemical shifts range from 7.48 ppm for [7]cycloparaphenylene to 7.71 ppm for [18]cpp[25], shifting downfield with size. The proton chemical shift of [6]cycloparaphenylene is the only exception to this trend at 7.64 ppm[21].

Using these characteristic peaks and a mixture of sizes, Yamago was able to demonstrate with that [10]cycloparaphenylene hosts C_{60} whereas [9]- and [11]cpp do not[26].

In this report, a variable temperature study is performed that shows the chemical shift of [10]cycloparaphenylene moves upfield with decreasing temperature. Since the signal of [10]cpp remains a singlet at -80 °C while also constrained by a contained C_{60} it "must be structurally flexible and rapidly fluttering". Jasti has recently reported a crystal structure for this complex[24].

The crystals of cycloparaphenylenes (Figure 7) generally exhibit a "herring bone"

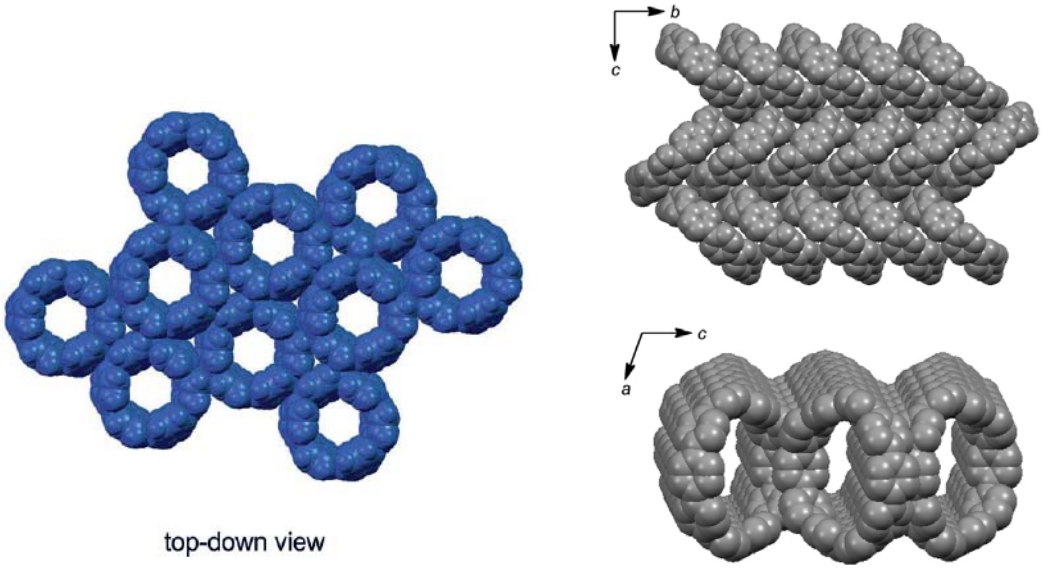

Figure 7. Crystal structures of [6]cycloparaphenylene[21] (left) and [10]cycloparaphenylene[27] (right).

style packing and frequently include disordered solvent molecules within the hoop[16,28,27]. For most hoop sizes, the individual phenyl rings are canted with dihedral angles of ~30°. The crystal structure of [6]cycloparaphenylene, however, shows the phenyl units are non-planar and aligned with the cylinder of the molecular hoop[21]. The packing structure is perfectly

cylindrical, forming carbon nanotube-like arrangements. In all reported cases, crystals of cycloparaphenylenes have tubular channels.

Theoretical Computation

Cycloparaphenylene has been the subject of computational investigation since carbon nanotubes were elucidated in the 1990's[29]. Since their synthesis, many more computational studies have been published in an effort to explain the unexpected optical properties observed in this class of molecules. These studies have produced a diverging set of explanations ranging from exciton localization to more conventional descriptions of molecular orbital transitions.

Jasti includes DFT (PBE GGA) results with his initial synthetic publication indicating even numbered cycloparaphenylenes favor a staggered arrangement, with every other phenyl tilting in or out of the cylinder of the molecule with a consistent dihedral angle (no symmetry specified), whereas odd numbered cpps have irregular dihedral angles (C_2 axis specified)[17].

Wong (using PBE0) also finds staggered conformations, reporting even sizes [12] and lower converge to C_{2v} symmetry and the larger sizes converge to lower symmetries[30]. The average dihedral angles he reports generally increase with size (approaching the linear paraphenylenes), but many of the values break this trend, particularly when compared within a narrow size range (e.g. [8]cpp=32°, [10]cpp=26°.). He describes an "electronic competition" between a delocalized, quinoidal form and a phenyl-localized, benzenoid structure and concludes that "a complete analysis of the conformational landscape available to the nanorings is beyond the scope of this work."

Sundholm, Taubert and Pichierri published a study (DFT BP86 GGA) including [6]-[11]cycloparaphenylene and found energy minimum conformations that also included canting of the phenyl units, breaking cylindrical alignment and lowering symmetry ([6]-[11]cpp: D_{3d}, C_2, D_{4d}, C_2, C_s, C_1)[31]. They also optimize the excited state geometries, finding significant double bond character in the phenyl-phenyl bonds and "pronounced qunioid

character" for the smaller hoops. They conclude "it is not obvious that the optimized molecular structures are the energetically lowest conformations".

Grasping these issues, Itami published a study looking exclusively at the interplay of strain and structure. Using DFT at the B3LYP/6-31G(d) level, they find the same energy minimum conformations for the even numbered cycloparaphenylenes described by Jasti: regular, alternating phenyls with angles around 33°, and extend Jasti's description of the conformations of the odd numbered cpps by noting they contain a single three-membered helical arrangement amongst the otherwise alternating phenyls[32]. They then calculated the energies of fourteen additional conformations of [12]cpp with different arrangements of helical and alternating phenyl sets. The conformations with one set of helically arranged phenyls were close in energy to the alternating form (ΔG=1.5-2.2 kcal·mol^{-1}). Calculations for the transition state between the all-alternating form and one with a single, helical phenyl set resulted in a lowest energy barrier of 3.8 kcal·mol^{-1}. They conclude that the phenyl rings in [12]cpp rotate "rather freely" at standard conditions, implying that the observed optical properties result from a dynamic mixture of different rotational conformations.

Yamago includes his first computational contribution within his second synthetic paper, verifying the structure and energy calculations of Itami and reporting for the first time the HOMO-1, HOMO, LUMO, and LUMO+1 energies for [4]-[20]cycloparaphenylene[25]. He finds, contrary to the trends in the linear paraphenylenes, the HOMO increases with size while the LUMO decreases with size. The HOMO-1 and LUMO+1 are reported to be doubly degenerate and follow reverse trends, so the HOMO-1 decreases along with the LUMO and the LUMO-1 increases with the HOMO. Using TDDFT, they conclude that the HOMO→LUMO transition is forbidden, having little to no oscillator strength, while the HOMO-1→LUMO (and degenerate HOMO-2→LUMO) and HOMO→LUMO+1 (and HOMO→LUMO+2) do have strong oscillator strengths (Figure 8). They then assign the size-independent absorption maximum to these transitions, since the orbitals involved shift equally with size, maintaining a constant gap (Figure 9).

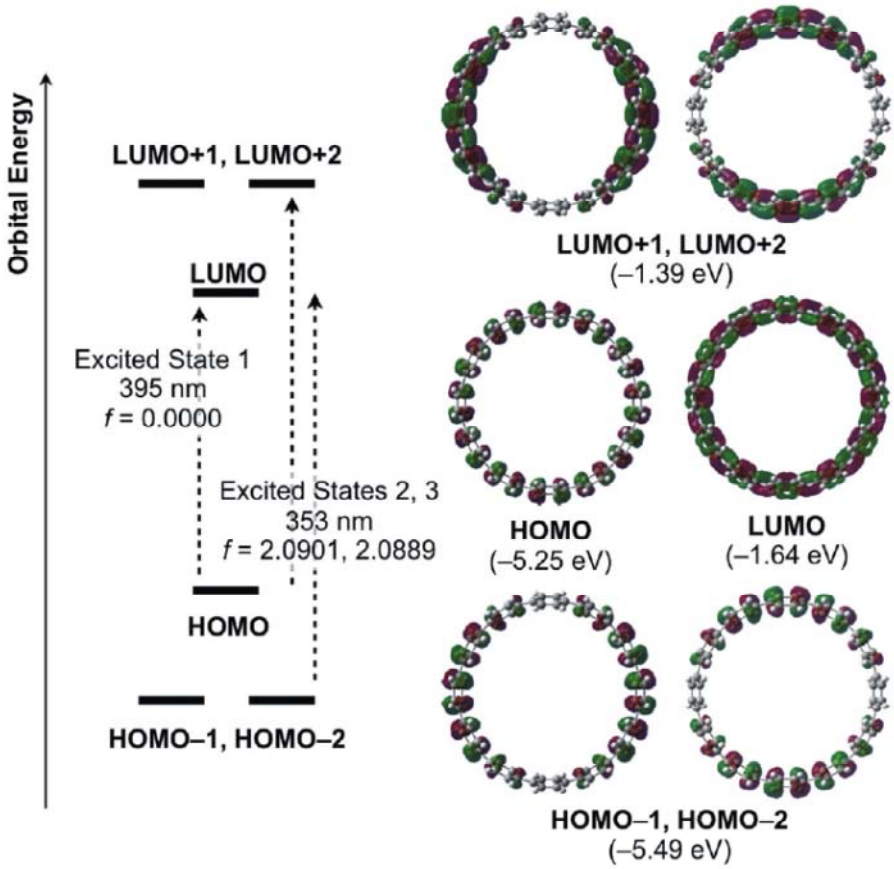

Figure 8. Frontier orbital diagram, energies, and proposed absorption transitions of [12]cpp[32].

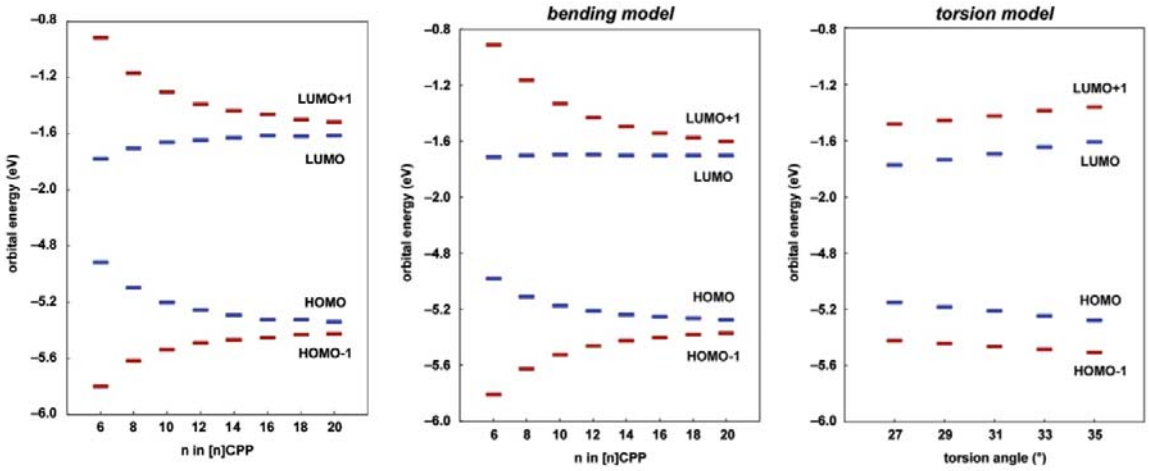

Figure 9. Frontier orbital trends with hoop size (geometry optimized, left), hoop size (torsions locked at 31°, middle) and torsions locked at X° for [12]cycloparaphenylene[32].

The following year, in their publications of [7]cycloparaphenylene[20] and [6]cpp[21], Jasti's group reproduced similar TDDFT calculations, verifying and reiterating Yamago's conclusions. In addition, they note a weak sideband in the absorption spectra of [7]cpp might be a weakly allowed HOMO→LUMO transition.

Most recently, Itami has extended Yamago's explanation of the absorption and fluorescence spectra by calculating the excitation wavelengths for the relevant transitions (HOMO→LUMO+1, etc.) and further exploring the effects rotational isomerization may have with respect to these orbitals[33]. The excitation wavelengths of the HOMO→LUMO+1 type transitions are shown to closely match experiment (ranging 326-362 nm vs. the experimental 339 nm) whereas the HOMO→LUMO transitions are calculated to be wider ranging and inversely proportional to size (491-379 nm for [6]-[20]cpp). Furthermore, the calculated oscillator strengths for the HOMO→LUMO transition are consistently zero and range 0.78-4.01 for the HOMO→LUMO+1 type transitions. Next, Itami considers the effect phenyl-phenyl torsions and phenyl out-of-plane bending have on the orbitals of interest (Figure 10). He calculates the orbital energies for [8]-[20]cpp with the phenyl-phenyl

torsions set to a constant 31°, finding the primary effect is to make the LUMO energies hoop-size independent (whereas normally the LUMO is proportional to hoop size). Itami proposes that in keeping the torsion angles constant, the effect of out-of-plane bending within each phenyl can be observed. The results indicate that the LUMO energy is independent of this bending. Finally, he calculates the orbital energies for a series of [12]cpp conformations with the torsion angles for every phenyl set to constant values ranging from 27-35°. The relevant frontier orbitals are shown to trend linearly with torsion angle, with the LUMO and LUMO+1 increasing in energy with increasing torsion angle and the HOMO and HOMO-1 energies decreasing with increasing torsion angle (Figure 10). Although he doesn't use the word "quinoid", he ascribes these observations to the phenyl-phenyl double bond character in the LUMO being more sensitive to the orbital overlap dictated by torsion angle than the phenyl localized HOMO.

The overall picture one gets can be summarized as a competition between the extremes of hoop size. In the infinite-hoop limit, the molecule behaves as the linear paraphenylenes, with each phenyl exhibiting benzenoid character and phenyl-phenyl torsions (~37°) minimizing steric interactions of ortho hydrogens and electron density between phenyls. In the small-hoop limit we have a few examples to choose from. The photodimer of anthracene is formed with a loss of aromaticity in the central ring and the formation of two double bonds at the para positions, resulting in a quinoid structure. This might be considered a substituted [2]cycloparaphenylene. The early computational study with [5]cycloparaphenylene provides another example, where the authors found a quinoid form for the optimized structure[29]. For all sizes, it is apparent from the calculated orbital shapes that the HOMO represents the benzeneoid form while the LUMO is quinoidal. The energy of the HOMO is therefore dependent on phenyl bending that weakens the local benzeneoid aromaticity of each subunit; the HOMO varies primarily with the size of the hoop. The energy of the LUMO depends on the torsion angle because the phenyl-phenyl double bond character is proportional to the overlap of atomic p orbitals. Finally, the multiplicity of

energetically accessible rotamers suggests a continuum or a gradient manifold of orbital energies, especially for the LUMO, in any real sample.

Discussion. Our interest in cycloparaphenylene originated from the fact there are no known examples of a highly coordinated metal bond to a carbon nanotube. A metal bond to cycloparaphenylene might provide an interesting analog to metal-CNT complex, allowing investigation of the electron transfer through such a structure and determination of its photophysical properties. Itami's route, with the highest overall yield available, provided our first work towards this goal (Scheme 1).

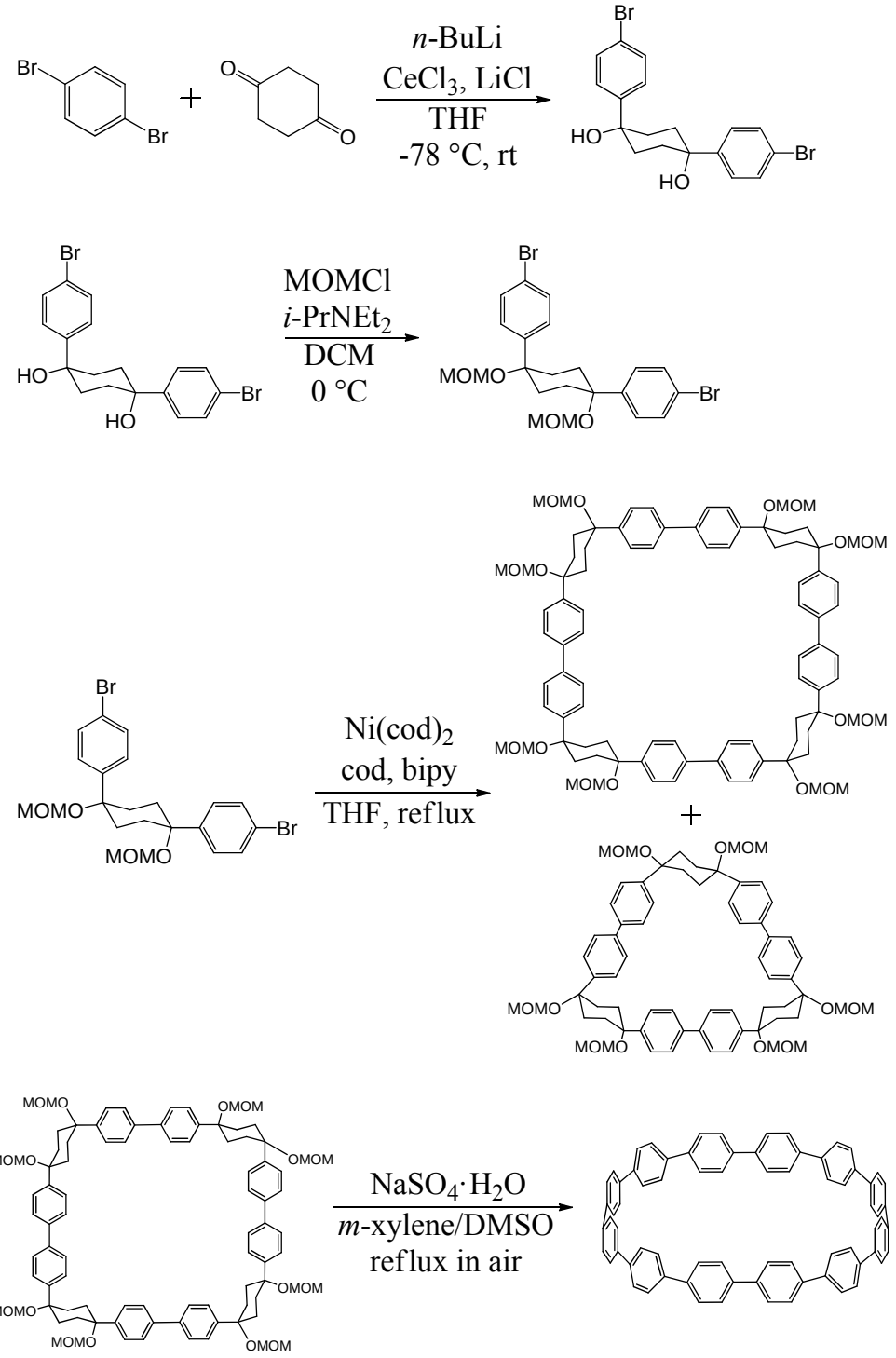

Scheme 1. The reactions composing Itami's synthesis of cycloparaphenylene.

An early problem encountered was the convoluted final aromatization step. This reaction is composed of multiple steps that Itami summarizes as MOM deprotection, dehydration and aromatization. Deprotection is achieved with specific quantities of aqueous tosyl alcohol or sodium bisulfate monohydrate (implicating a stoichiometric amount of water). Additionally, DMSO is used as a cosolvent that Itami speculates "stabilizes a high-energy intermediate". Difficulty in reproducing this final step and lack of a clear description of the reaction mechanism ultimately led us to using Jasti's route after he published the gram scale paper.

However, investigation of apparent side products led to the discovery that Itami's route produced variable sized nanohoops. NMR spectra showed a single peak in the aryl region at 7.67 ppm and the characteristic double peaked fluorescence spectra matched [15]cycloparaphenylene. Itami had not described his macrocyclization reaction as producing a penta-mer that would go to [15]cpp. Other analysis showed peaks that looked like [12]cpp (7.61 ppm) or [9]cpp (7.52 ppm) in addition to the peak for [15]cpp. This was confusing because the macrocycle precursor for the final step seemed pure by NMR.

Review of the reported NMR spectra revealed the trimer and tetramer macrocycles, for the previously reported [9]cpp and [12]cpp precursors, were reported in different solvents, preventing direct comparison of the spectra. It was also noted that Itami had recrystalized his macrocycle before the final step. We propose that we must have a mixture of macrocycles, along with other oligomer products, that were nearly indistinguishable by NMR before the final aromatization step. Column chromatography was performed on the crude product of the nickel coupling reaction that produces the macrocycles, carefully fractioning.

NMR spectra of select fractions were nearly identical, with the exception of the MOM groups (Figure 10). The fastest eluting macrocycle matched the trimer macrocycle

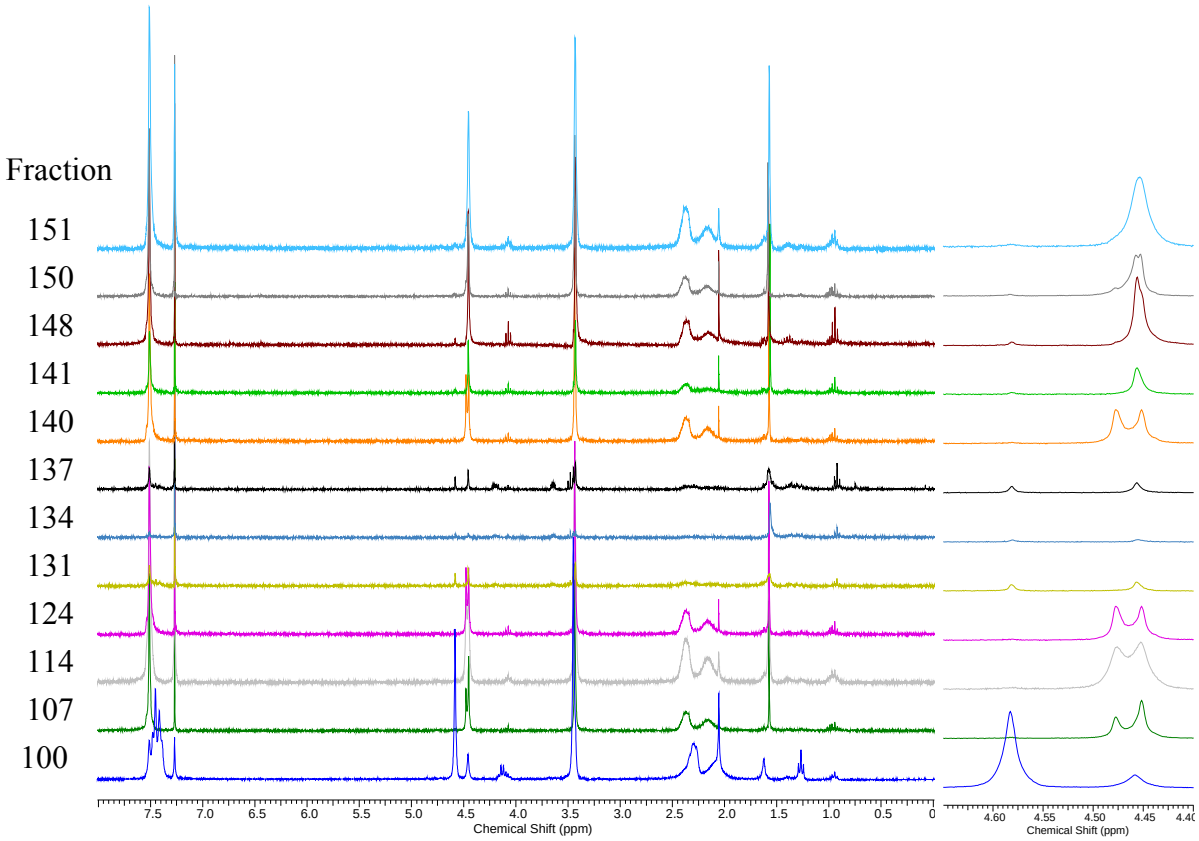

Figure 10. ^{1}H NMR spectra of select macrocycle fractions (y-axis) normalized by intensity of the solvent peak. The right shows the region of the MOM methyl peaks that shift most for the different macrocycle sizes.

reported by Itami that produces [9]cpp, based on the more downfield MOM peak. The other fractions appeared at first like the tetramer, but closer examination showed a small but definite shift in the MOM peak. By comparing the NMR spectra from a series of eluted fractions we were able to identify four unique macrocycles.

Select fractions from the above macrocyclization reactions were carried forward to the final aromatization step. These reactions produced sets of peaks matching the reported peaks of [9]-, [12]-, [15]- and [18]cycloparaphenylene (Figure 11). The difference of three phenyls between the resulting hoops is consistent with the fact that the macrocycles are

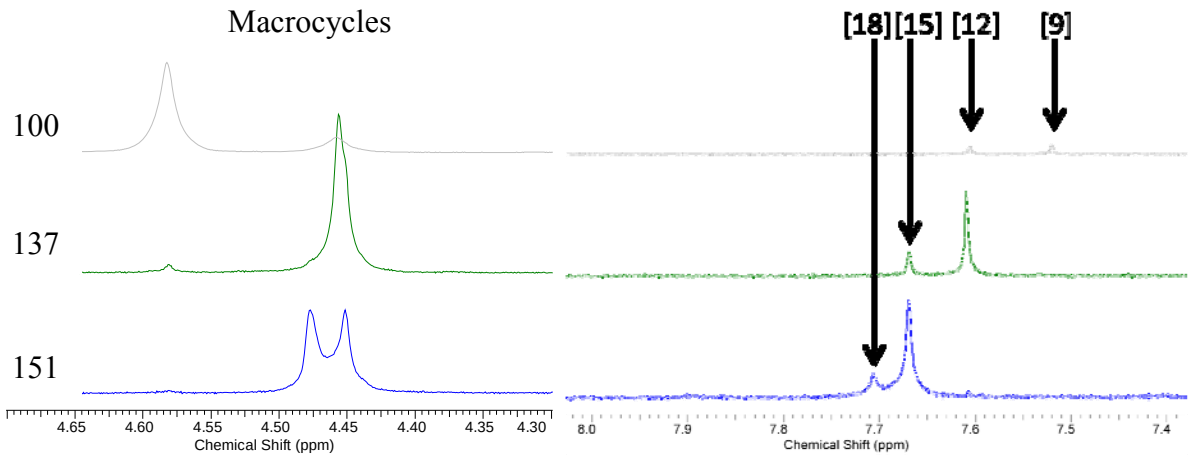

Figure 11. ^{1}H NMR spectra illustrating the correlation of macrocycle MOM methyl peak (left) and resulting cycloparaphenylene size (right) for select fractions. Cycloparaphenylene peaks corresponding to [9]-, [12]-, [15]- and [18]cycloparaphenylene can be seen from right to left.

composed of "masked" terphenyls. These results show that the nickel coupling system is more dynamic than Itami described.

During the coupling reaction many different intermediate coupling products are generated. Each L-unit must be first coupled to form a dimer, but then the dimer can be coupled to either a "masked" L-unit monomer or another dimer, producing either a trimer or tetramer. Then any of those four can couple with any other, producing up to an octomer. The distribution of the products must be based on the relative rates of each specific form, the concentration of each form over time and the solubility limit for longer oligormers. To complete the macrocycles the termini must be coupled, which will have another set of rates. Although the reaction starts with the coupling of a single species, it almost instantly becomes

a mixture of different *p*-bromo aryl compounds. Therefore, a specific *p*-bromo aryl could be added to produce a substituted cycloparaphenylene.

New nickel coupling reactions were performed with the addition of *p*-dibromobenzene. We call this variable coupling. The macrocycles produced were, as before, seemingly indistinguishable by NMR. A second NMR experiment with the sweep width set to the MOM range and a greater number of transients showed multiple peaks in this area that looked promising (Figure 12), but other peaks in the crude and lack of similarly resolved

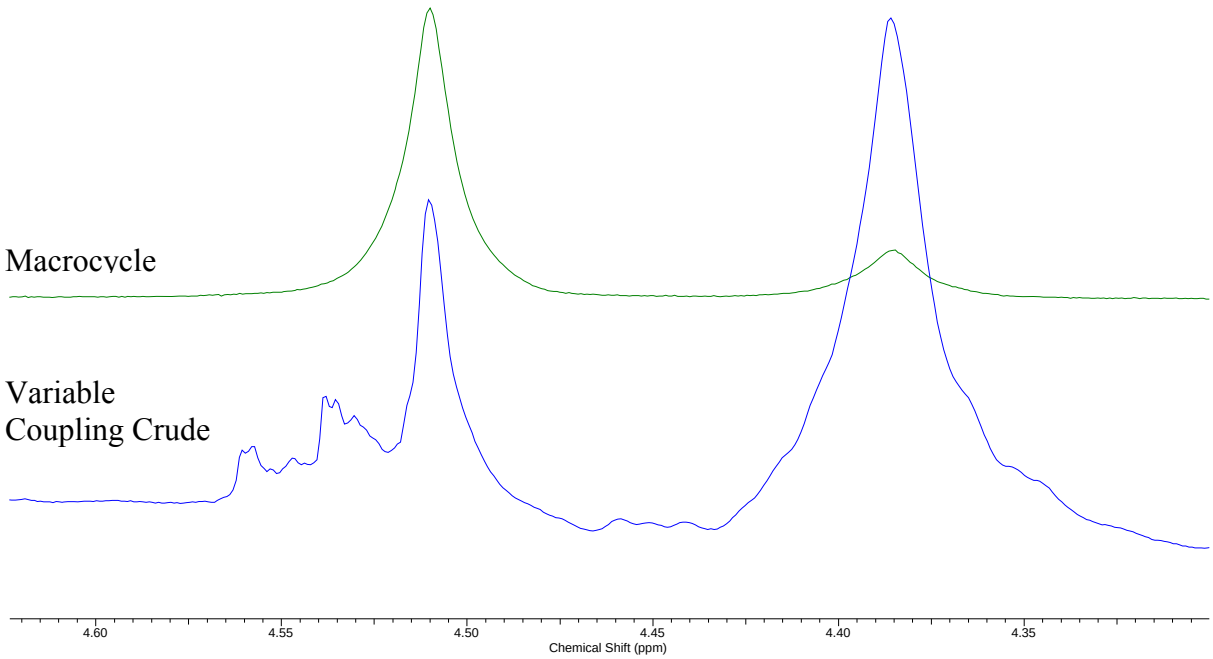

Figure 12. ^{1}H NMR spectra of the MOM methyl region for fraction 100 of finely fractioned macrocycle (top) and crude variable coupling product (bottom) illustrating appearance of new macrocyclization product peaks.

spectra from the previous couplings made this inconclusive. The crude macrocycle was again fractioned by column and multiple final step reactions with various fractions were performed.

The NMR spectra of the aromatized macrocycles were instantly convincing. Each fractioned contained a few peaks that exactly matched different sizes of cycloparaphenylene in the expected size range. The earlier fractions contained peaks for [9]-[13]cpp (Figure 13)

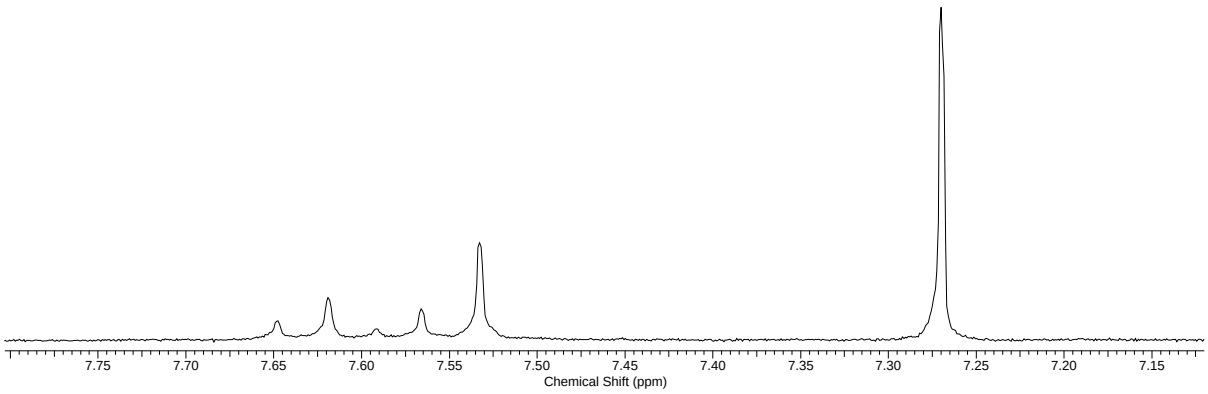

Figure 13. ^{1}H NMR spectra of the cycloparaphenylene region for variable coupling fraction after final aromatization reaction and workup. Separate peaks corresponding to [9]-[13]cycloparaphenylene are seen between 7.50 ppm and 7.70 ppm.

and the later fractions [12]-[16]cpp. Each independent fraction shows different integration areas for the peaks, demonstrating that these peaks correspond to separate molecules in solution.

The distribution of sizes was estimated by normalizing the peak height of [9]cpp (the tallest) to 1, the other heights were then 0.370, 0.133, 0.387, 0.176 for [10]-[13]cpp. The initial concentration of the *p*-dibromobenzene was 1/8th that of the L-Unit. Although there are multiple ways to form the different sizes, generally [9]cpp should have no dependence on the dibromobenzene concentration, [10]cpp should have a first-order dependence and [11]cpp should have a second-order dependence. The trends in the distribution are consistent with this estimate.

The reaction conditions of the variable coupling were further explored. The explored conditions include a control reaction without a second aryl, different relative concentrations of dibromobenzene to the L-unit, different concentrations of both (i.e. dilute or concentrated systems), and finally diiodobenzene instead of dibromobenzene as the variable aryl unit. The crude products were separated into a few fractions and set up as separate aromatization reactions. The resulting sets of macrocycle "fractions" were characterized based on the resulting sizes of cycloparaphenylene (Figure 14); that is, the resulting cpp population should correlate to macrocycle population produced from a given set of coupling parameters.

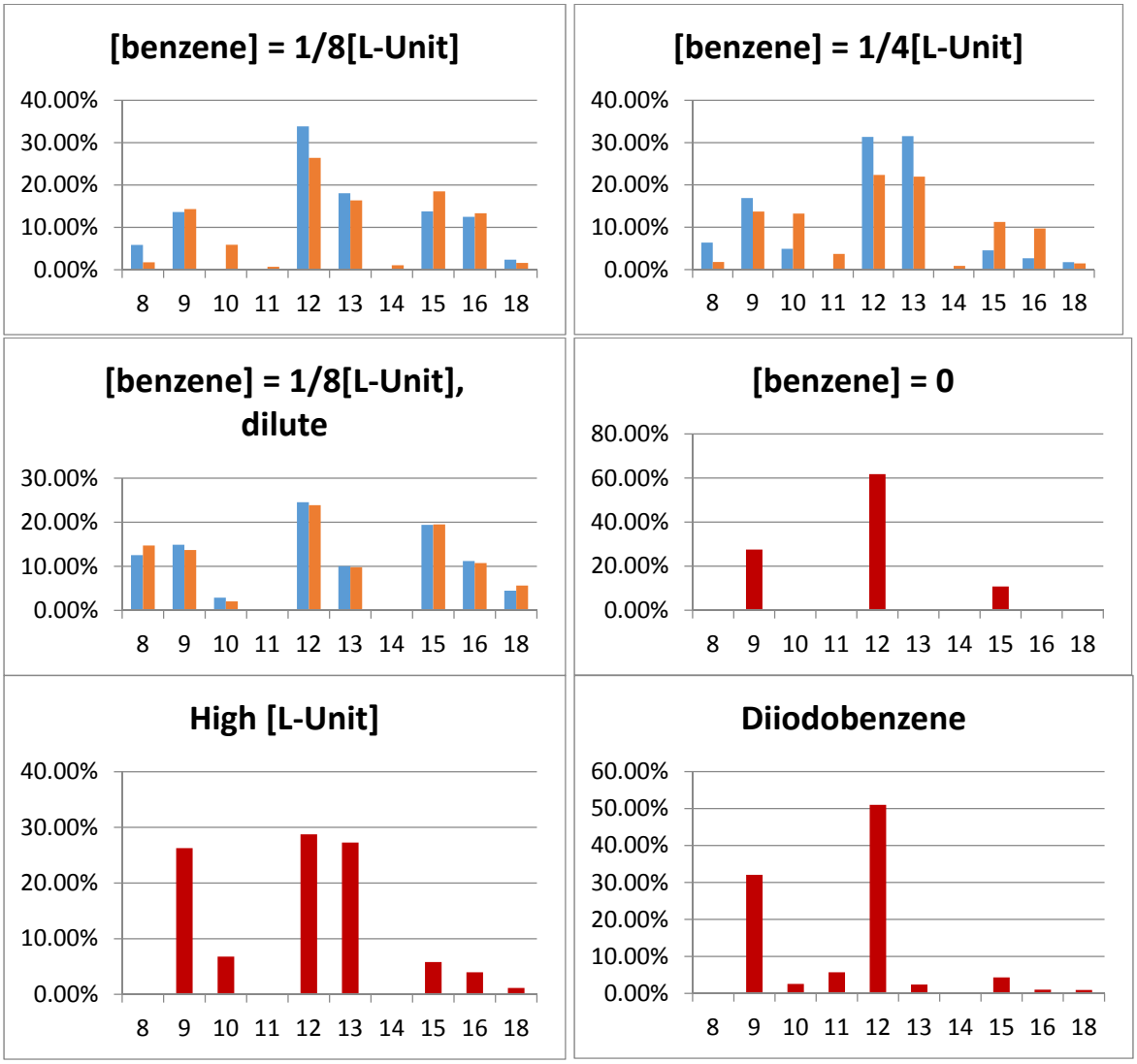

Figure 14. Distributions of cycloparaphenylene sizes (x-axis) for nickel coupling reactions under different conditions, expressed as a percentage of total cycloparaphenylene mass (y-axis). The red represents the sum of masses calculated from multiple spectra of separate fractions (Figure 15). The blue represents the masses calculated from one spectrum after the separate fractions were combined.

The yields for each separate fraction were calculated with an internal standard (Figure 15), following which the "fractions" were recombined, and the yields calculated again to

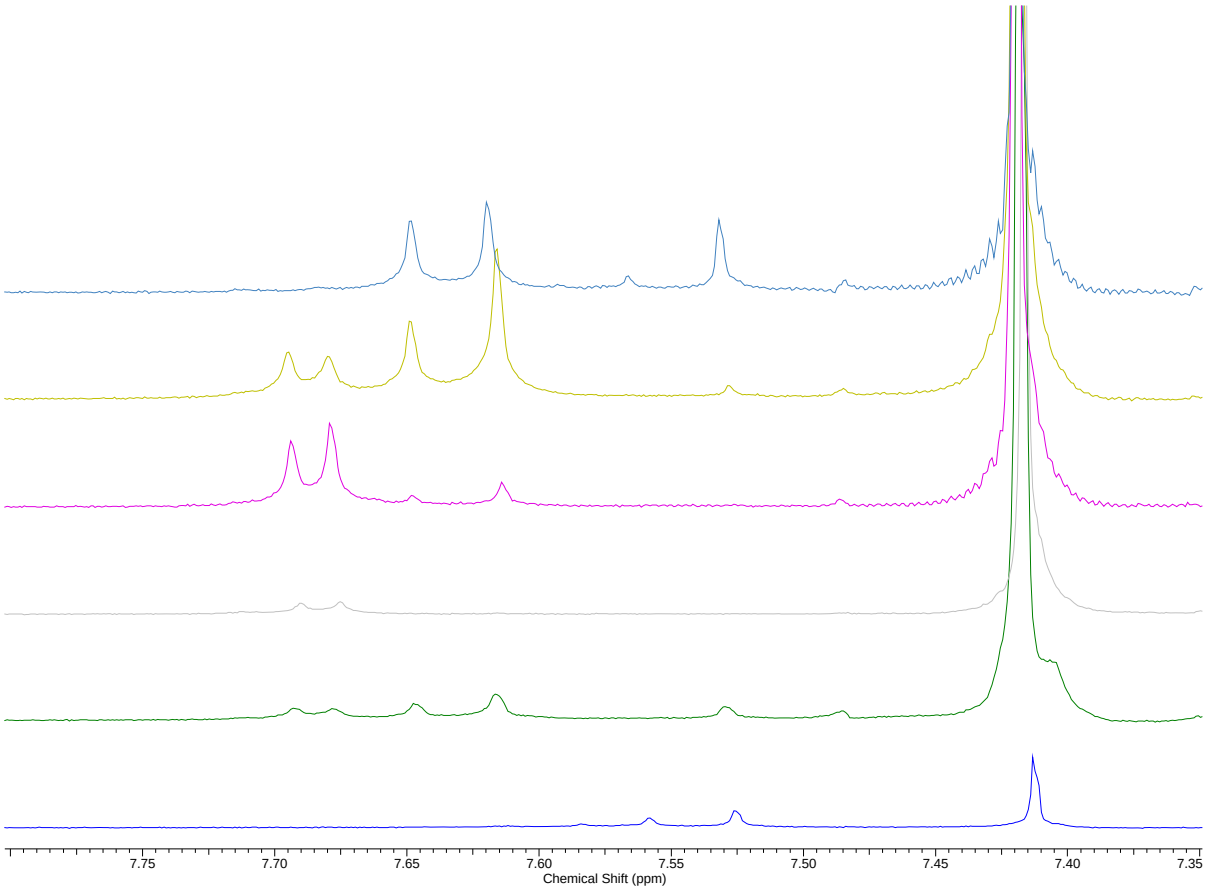

Figure 15. ^{1}H NMR spectra of the cycloparaphenylene region for fractions of a variable macrocyclization trial after final aromatization reaction and workup. The integration areas were converted to masses and summed to produce the data in Figure 16. The large peak on the right is the diiodobenzene internal standard.

provide a sense of the reproducibility of the method. In some cases, smaller peaks were buried under the larger overlapping signals, seeming to eliminate them from the combined sample. Variance due to such overlapping and selection of integration areas makes the results somewhat less than quantitative. Additionally, analysis of this method with known quantities of p-diiodobenzene and bipyridine (~10 mg each) resulted in a standard deviation of 0.53 mg, the order of magnitude of the masses of the individual [x]cpp sizes. The calculated masses of individual sizes were converted into percentages of the total cpp mass, which should serve as a qualitative indicator of the distribution of macrocycles produced in the coupling reactions.

Review of the relevant literature revealed a number of possible metallation strategies. Of these, by far the easiest was the microwave generation of aryl chromium carbonyls[34] (Scheme 2) which involved a single step, few reagents, a short reaction time and

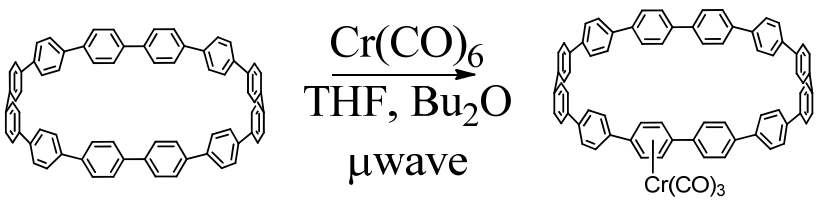

Scheme 2. Microwave driven formation of aryl chromium carbonyl[34].

which would be straightforward to characterize by the carbonyl IR stretching peaks. With an unexpected variety of cycloparaphenylene sizes in hand, we began a series of these chromium carbonyl reactions.

We produced carbonyl complexes with [9]-, [12]- and [15]cycloparaphenylene. ^{1}H NMR spectra of the yellow solids showed a small peak for the relevant cpp. The samples fluoresced weakly with the same colors as the unbound [x]cpp. After leaving an NMR tube in the mid afternoon sun the sample turned clear and the fluorescence of the sample increased in

intensity. These observations suggest that the chromium carbonyl complexes with cycloparaphenylene are both unstable to light and also quench its fluorescence.

The trends observed for the IR stretching peaks, which shift to higher energies with increasing cpp size (Figure 16), are consistent with the observed trends in the reported electrochemical data[25]. The electrochemical data show an increase in oxidation potential as the size of the ring increases, corresponding to a drop or stabilization of the HOMO energy. This same trend must then hold f[35]or the resulting molecular orbital arising from mixing of the HOMO orbital with the chromium orbital (Figure 17.) As size increases, electron density is less free to delocalize through the metal center into the CO antibonding LUMO, therefore resulting in stronger CO bonds with a higher stretching energy for the larger sized cycloparaphenylenes.

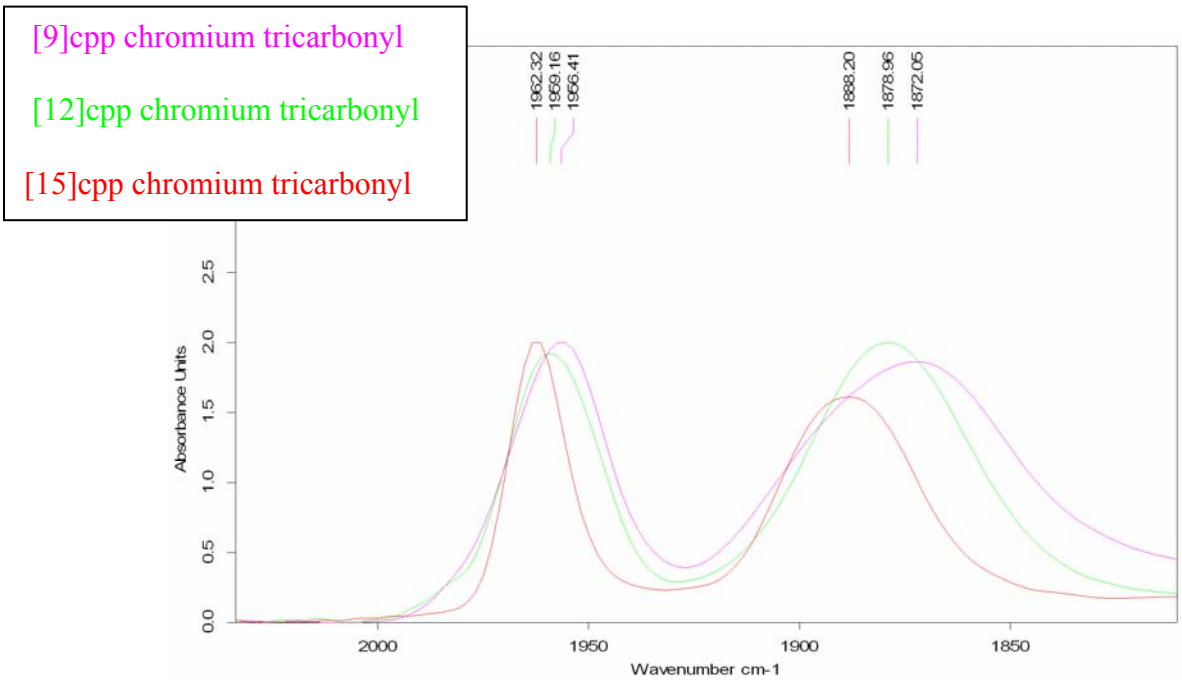

Figure 16. Normalized IR spectra of the carbonyl stretching region of [9]-, [12]- and [15]cycloparaphenylene chromium tricarbonyl.

Table 1. Peak maxima for the A_1 and E stretching bands of [x]cpp-chromium carbonyl complexes.

[X]cpp	**A_1**	**E**
[9]cpp	1956 cm^{-1}	1872 cm^{-1}
[12]cpp	1959 cm^{-1}	1878 cm^{-1}
[15]cpp	1962 cm^{-1}	1888 cm^{-1}

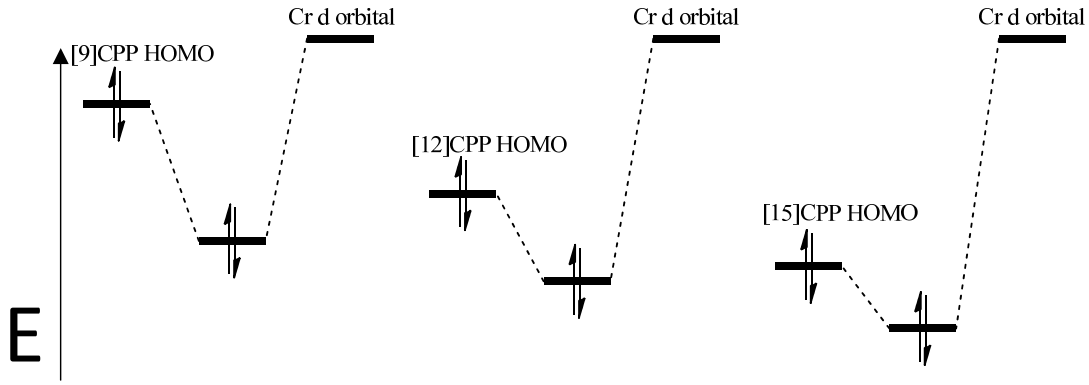

Figure 17. MO diagrams of [x]cpp-chromium complexes based on ordering of HOMO energies from electrochemical data.

Similar trials with molybdenum carbonyl and tungsten carbonyl have been performed. The molybdenum trials produce no product; the crude was clear and contained black solids, perhaps metallic molybdenum. The IR of the dried molybdenum crude showed no carbonyl peaks. The tungsten did produce yellow solutions, but the IR lacked carbonyl stretches. This yellow product was light stable even after a period of weeks in sunlight.

Aside from the metal carbonyls, brief efforts were made with an iron-arene exchange reaction (Scheme 3), which was light driven. No products were isolated on workup, but a red-brown stain was observed on the bottom of the reaction vessel, likely decomposed iron.

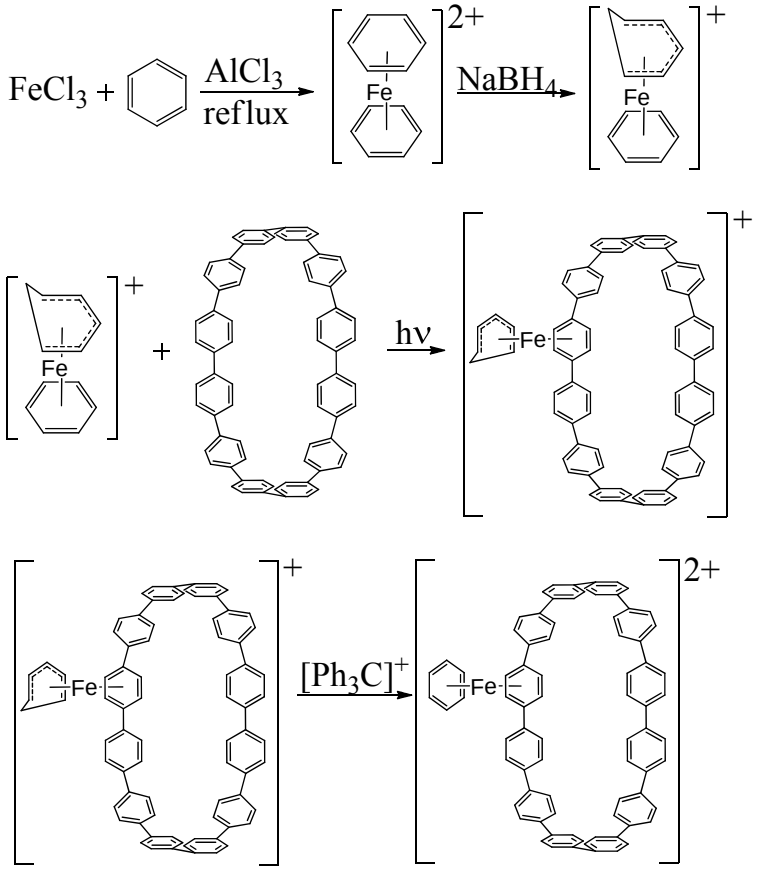

Scheme 3. Light driven arene exchange from cyclohexadiene iron complex[36].

Following these efforts we switched to Jasti's gram scale synthesis[24]. We found difficulties with two steps, one of which was ultimately determined to be light sensitive, the

other was temperature sensitive (Scheme 4). While working through these difficulties we discovered a new carbon-carbon coupling reaction, the focus of Chapter 2.

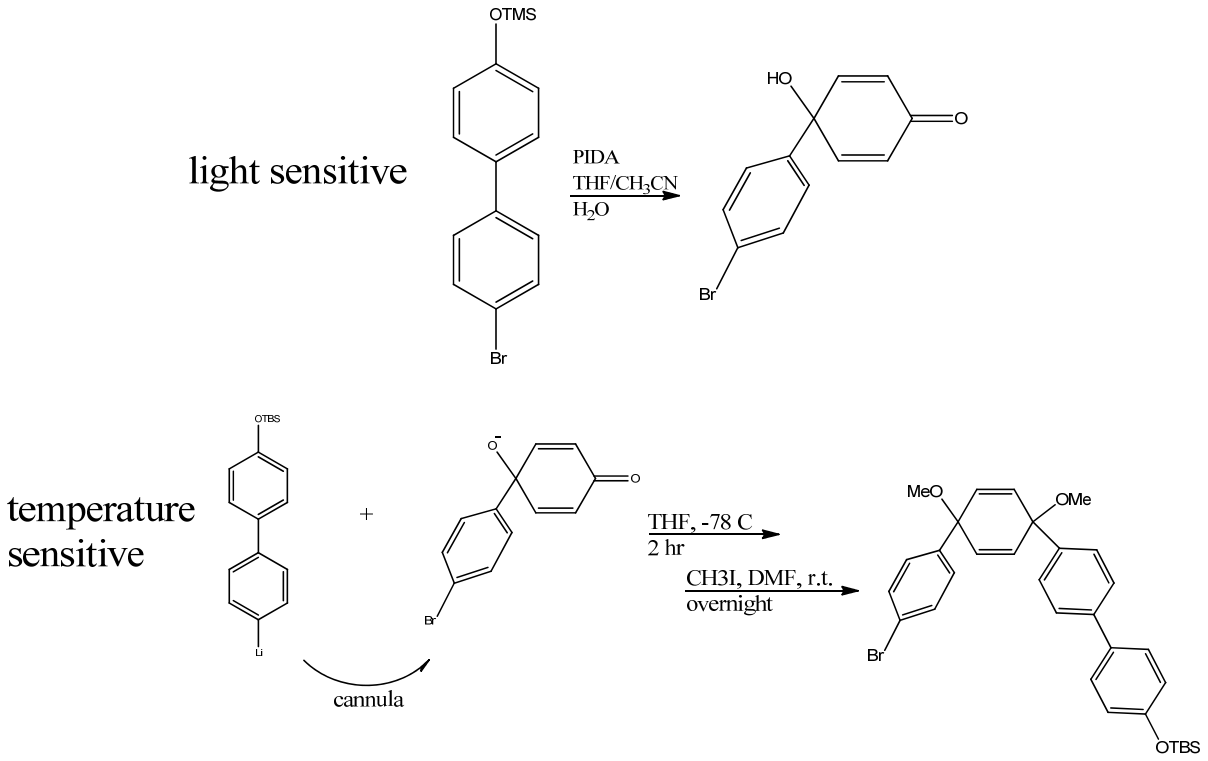

Scheme 4. Light and temperature sensitive steps in Jasti's gram scale synthesis of cycloparaphenylene.[24]

CHAPTER 2

Abstract. New coupling reactions with metal carbonyl reagents and substrates containing carbonyl functionalities are reported. In some cases the McMurry product appears to be the major product. McMurry coupling is reviewed. Products identified by NMR, X-ray crystallography and/or LC-MS are reported.

Introduction. During our investigation of the thermal decomposition of phthalic anhydride with chromium carbonyl, in an effort to extend the bay region of linear paraphenylenes (biphenyl, terphenyl) by a Diels-Alder type reaction with the putative benzyne intermediate generated[37], we instead found substantial new C-C coupling products (Scheme 5). Some of

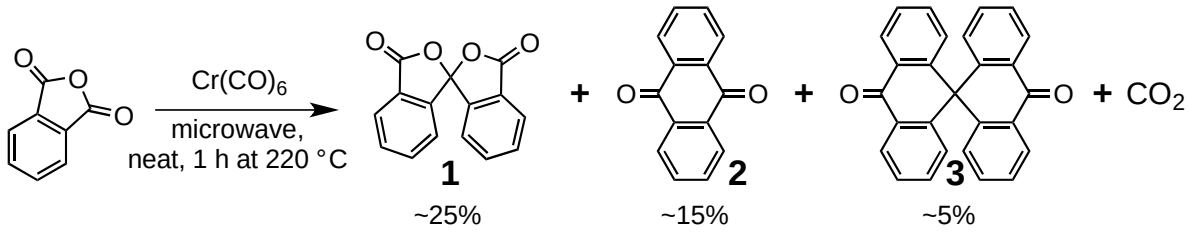

Scheme 5. Products identified from reaction of phthalic anhydride with chromium carbonyl. Yields estimated by intensity of NMR peaks.

these coupling products were spirocyclic in nature (1 and 3). Initial investigations of substrate scope revealed more modes of coupling, in the case of fluorenone producing the McMurry coupling product.

Background. McMurry coupling is the reductive coupling of ketones or aldehydes by zero or low valent titanium (Scheme 6)[38]. Zero or low valent titanium is generated in situ by a strong,

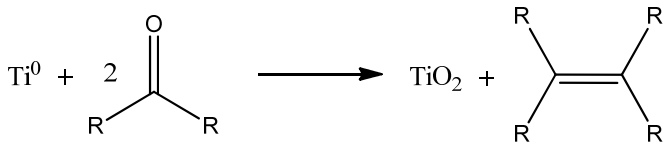

Scheme 6. McMurry coupling of a ketone.

stoichiometric reductant such as lithium, sodium, or other metal powder. The McMurry reaction is generally functional group tolerant and has been employed in a variety of strategies for synthesizing a wide variety of molecules including natural products, macromolecules, strained hydrocarbons and other alkenes difficult to access by other synthetic routes.

McMurry coupling was initially described by Tyrlik and Wolochowicz[39], and Mukaiyama and coworkers[40] then more broadly developed by John McMurry[41,38]. Fürstner has further developed the reaction into a catalytic system by addition of a chlorosilanes,

which convert titanium oxide byproducts back into the reactive, low valent titanium species[42].

The general mechanism of McMurry coupling is thought to involve a metallopinacol intermediate (Scheme 7). Although this has been the generally accepted view, based on the isolation of pinacols[43], carbenoid intermediates have also been proposed[44].

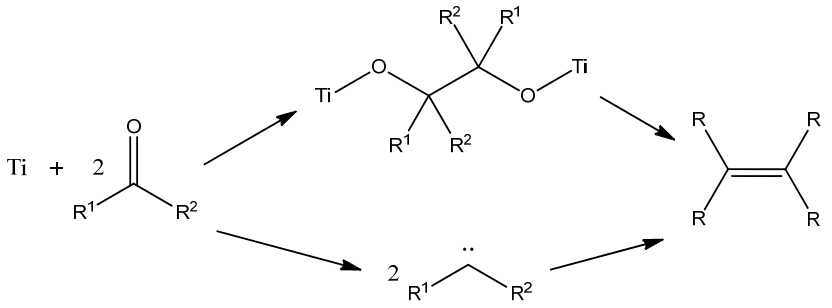

Scheme 7. Two possible intermediates in McMurry coupling: metallopinacol (top) and carbene (bottom).

A wide variety of natural products have been accessed by McMurry coupling. McMurry's first paper on the topic details the synthesis of β-carotene in one step from retinal in 85% yield (Scheme 8)[41]. McMurry coupling has been notably used in the total syntheses of (+)-compactin, mevinolin[45], crassin[46] and taxol[47] (Figure 18), among other natural products.

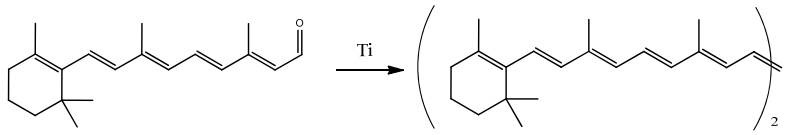

Scheme 8. One-step synthesis of β-carotene from retinal.

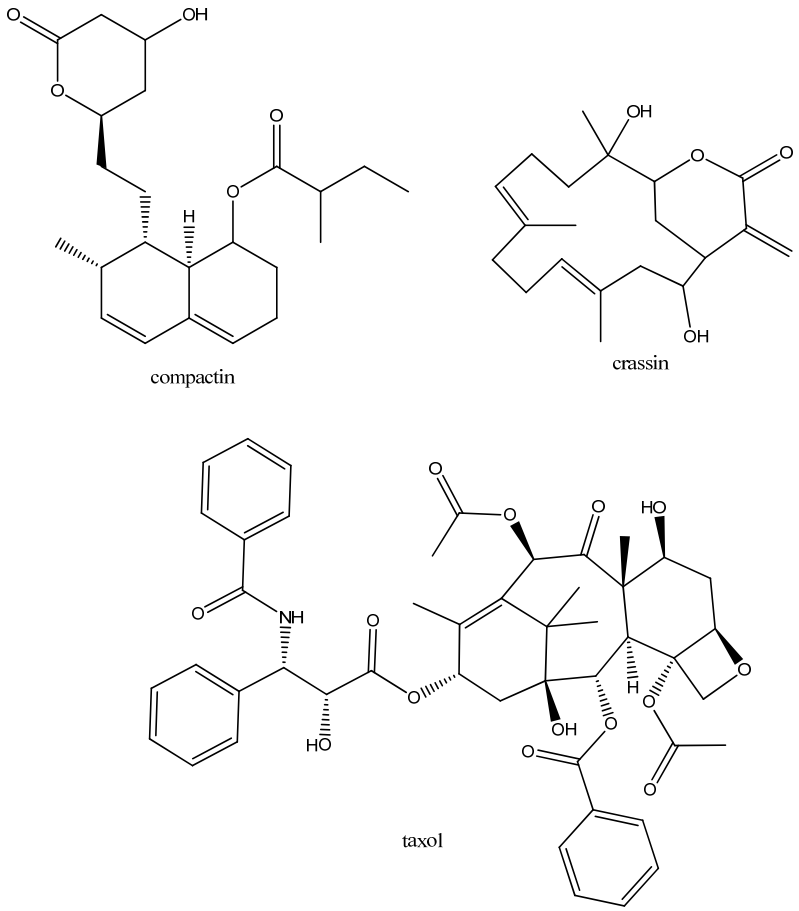

Figure 18. Examples of natural products synthesized in part by the McMurry reaction.

Aside from natural products, McMurry coupling has also been exploited in the synthesis of macrocyclic molecules. Iyoda published reports of large oligothiophenes accessed by McMurry coupling (Scheme 9)[48] which exhibit strong fluorescence with a large stokes shift. Kawase employed McMurry coupling in the formation of strained phenyl acetylene hoops and their derivatives (Figure 19)[49].

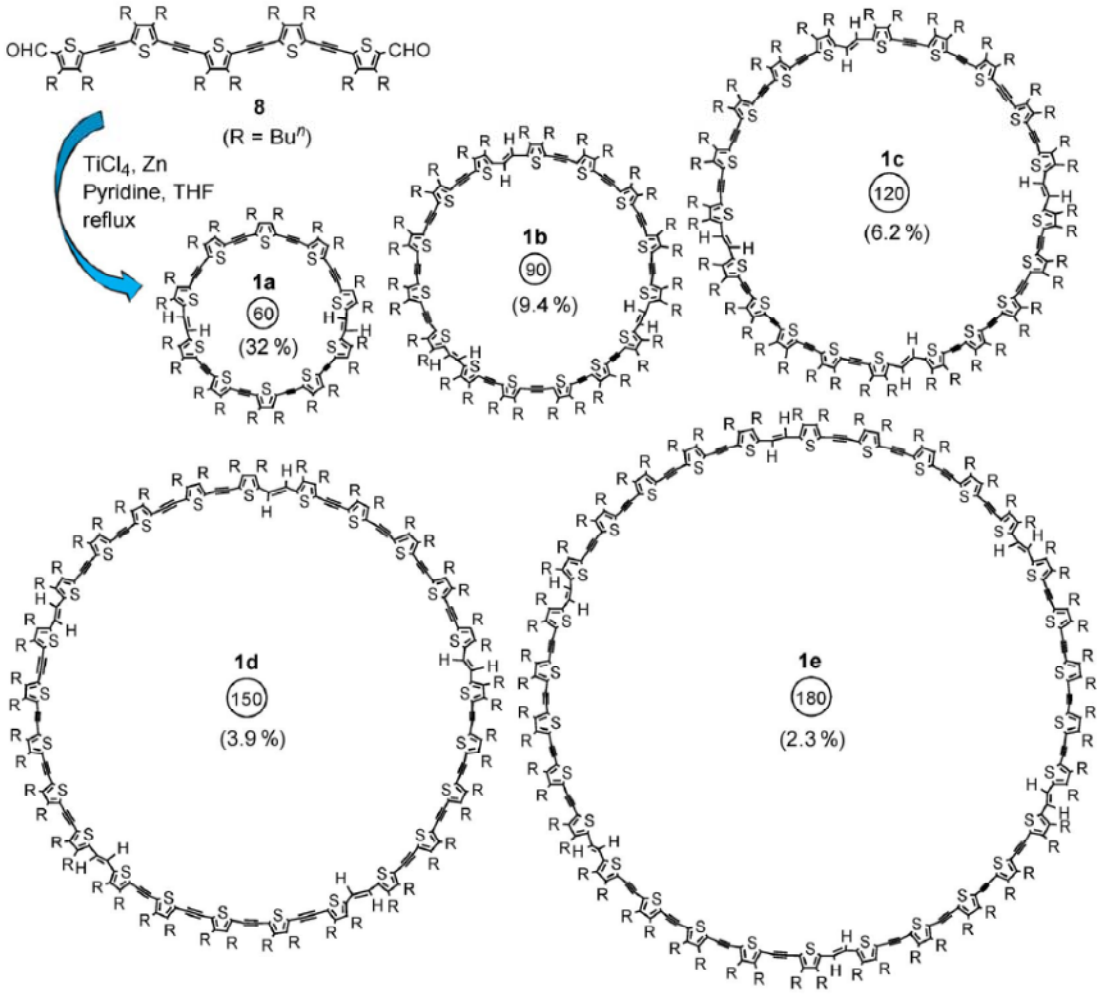

Scheme 9. Iyoda's large oligothiphenes accessed by McMurry coupling.[48]

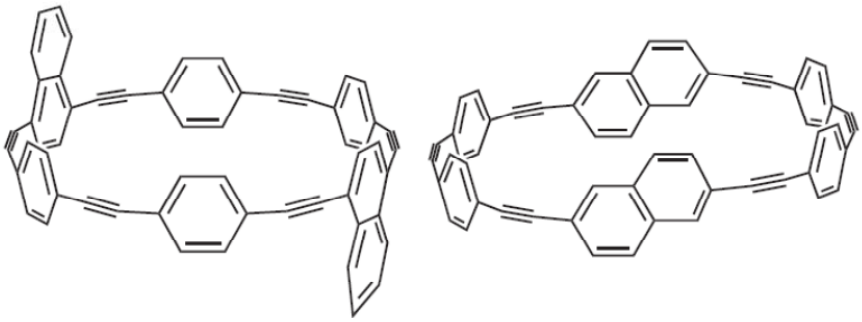

Figure 19. Examples of strained phenyl acetylenes Kawase produced using McMurry coupling[49].

McMurry coupling has also been of use in synthesizing strained hydrocarbons and functional carbon molecules. Dubois and Gingras synthesized 5-helicene by intramolecular McMurry coupling of a dialdehyde (Scheme 10)[50]. McMurry coupling was used in conjunction with other synthetic techniques to seal molecular hydrogen inside C_{60}[51]. Other applications include certain field effect transistors[52] and a light-driven molecular motor[53].

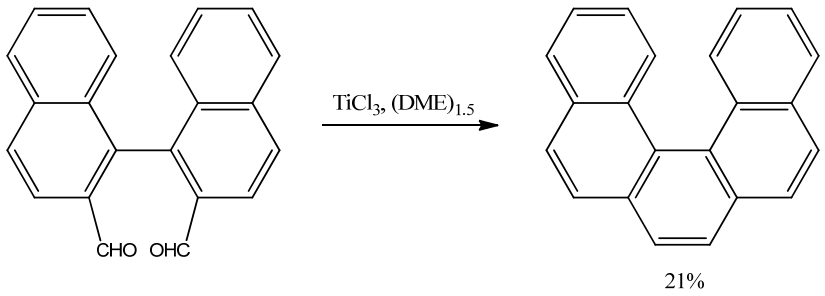

Scheme 10. 5-helicene formed by intramolecular McMurry coupling from dialdehyde precursor[50].

From these examples it is clear McMurry coupling is a versatile technique for organic transformations. It remains to be seen how similar our discovered reactivity is to the mechanisms described above. In the case of fluorenone, where the ketone is conformationally constrained, the product is the same, but in the other substrates, the products are unique. Discusssion. Our discovery of this new type of coupling began with pthalic anhydride. After heating phthalic anhydride with chromium carbonyl we were able to isolate various condensed polyaromatic molecules. The first such molecule, identified by x-ray crystallography, was the curious spirobisanthracene, the first time this molecule has been synthesized and the first time this class of molecule has been produced from a single synthetic step. Subsequent investigation of the crude product mixture showed substantial formation of a spirolactone and anthraquinone (Scheme 8). After these initial results, we sought to expand the substrate scope, in addition to trying other metals, to better understand the possible mechanisms involved.

Some preliminary investigations have been performed on all substrates shown in Figure 20. All substrates with moderate to low melting points produced new products by TLC. In all cases, excessive reaction time or temperature resulted in substantial formation of graphitic solid that has not yet been analyzed. Initial investigations of the products of these substrates by TLC (figure 21) and recrystallization have revealed various coupling products (Figure 22). In addition, LC-MS shows that in most cases a variety of new products have been formed. Substantial work still needs to be done with each substrate to determine ideal reaction conditions for yield and product selectivity.

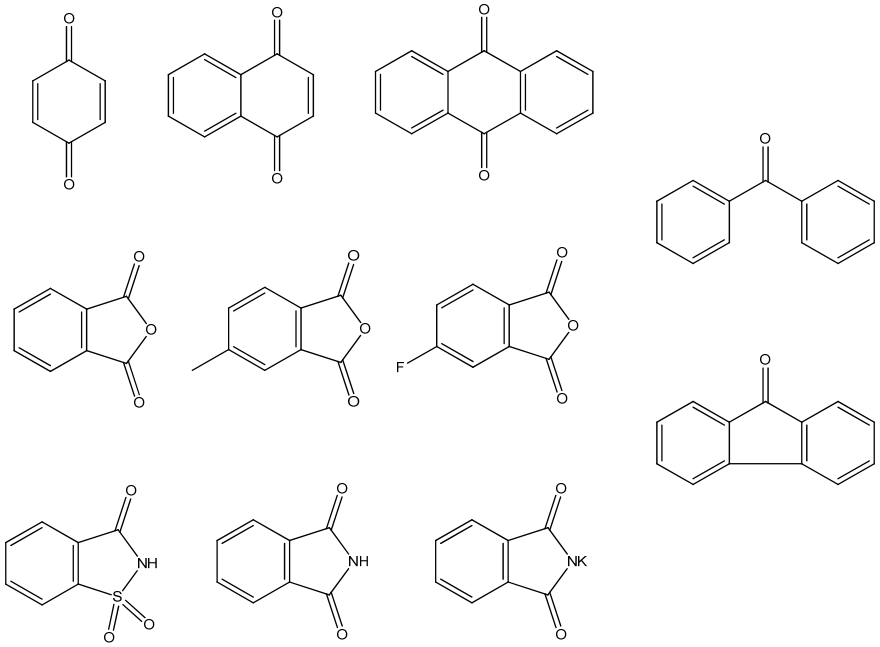

Figure 20. Substrates investigated for reaction with chromium carbonyl.

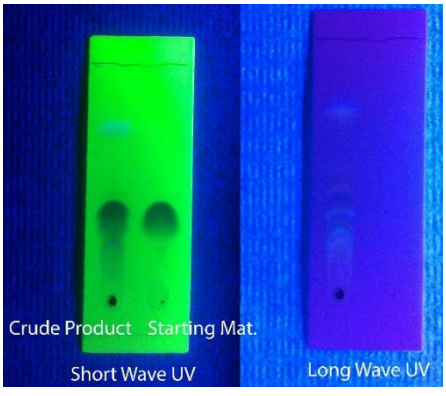

Figure 21. TLC of phthalic anhydride crude products vs. the starting material under short wave UV light (left) and long wave UV light (right).

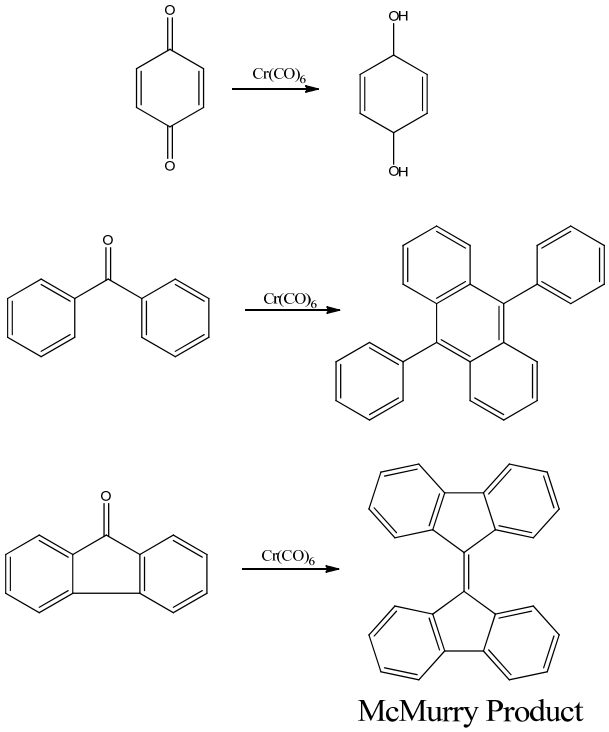

Figure 22. Additional products from microwave reactions with chromium carbonyl identified by x-ray crystallography.

In addition to various substrates, different metal carbonyls have been the subject of initial trials, to help elucidate mechanism. Preliminary LC-MS results and TLC show chromium carbonyl produces the greatest amounts of products, but products are also formed by iron, manganese and tungsten carbonyl.

Trials by microwave power were performed with 9-fluorenone. The effect of microwave power in this case is primarily the rate of heating (Figure 23). While the trial at 300 watts reaches the set point relatively quickly, the trial at 100 watts requires more time to reach the set point temperature of 250^0 C, spending more time in the ostensibly reactive temperature

range 200-250^0 C. The LC-MS results (Figure 24) show that in all three trials with 9-fluorenone and chromium carbonyl, the new products and amounts thereof remain relatively constant. In addition a reaction performed thermally, without microwave irradiation, showed similar results by LC-MS (Figure 25). These results lead us to believe there is no special "microwave effect" inherent to these reactions. Rather, the reaction arrives at an equilibrium state quickly above a certain temperature.

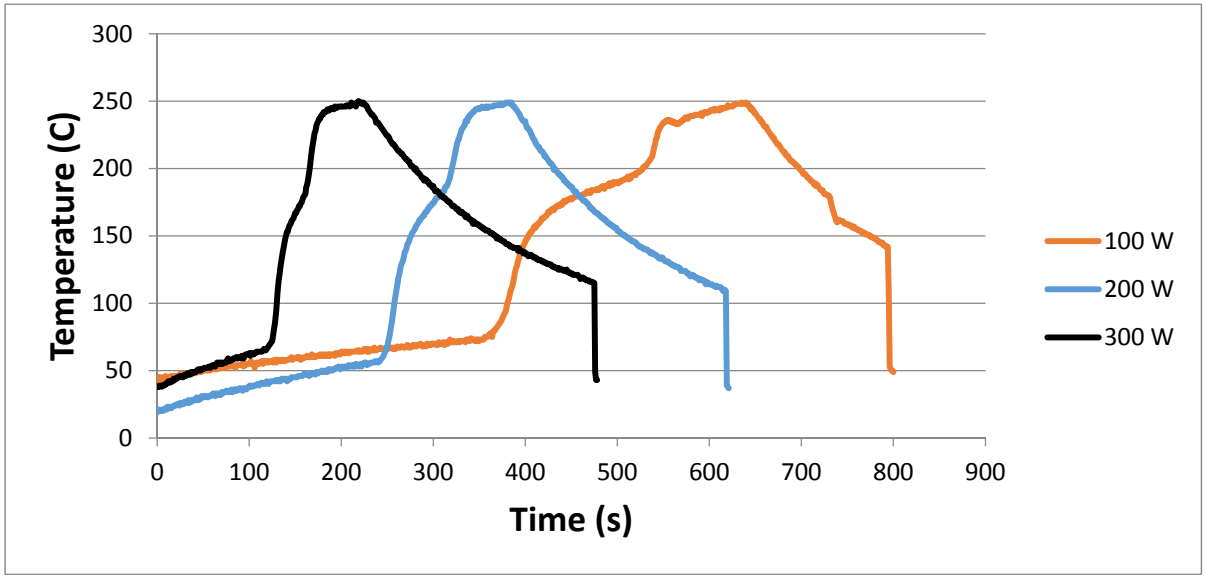

Figure 23. Tempearture profiles for microwave trials with 9-fluorenone. The lower power trials spend more time at reactive temperatures before the set point is reached.

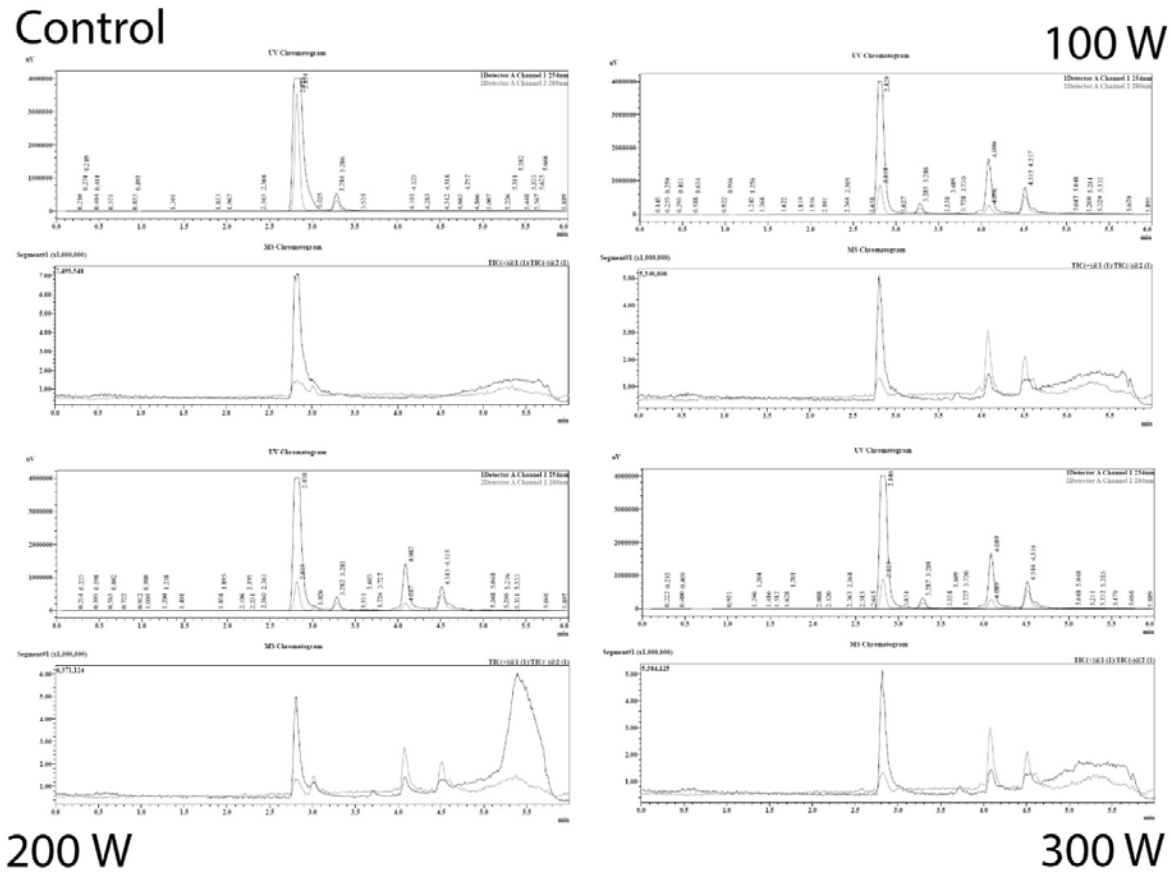

Figure 24. LC-MS chromatograms for trials with 9-fluorenone by microwave power. Within each set of spectra the UV Chromatogram is on top and the MS Chromatogram is on the bottom.

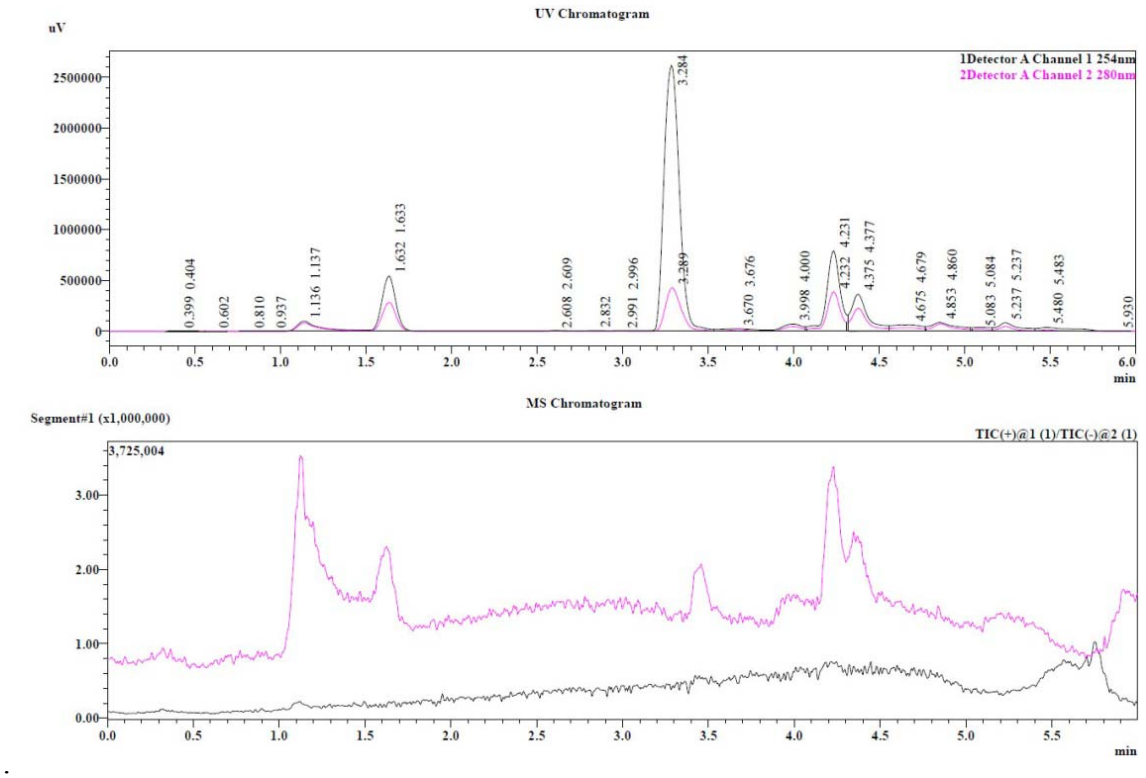

Figure 25. LC-MS of 9-fluorenone thermal reaction. Left two peaks in the UV Chromatogram are associated with starting material, center and right peaks are new products.

Trials with 9-fluorenone and chromium carbonyl also show stoichiometric consumption of the starting material. The MS chromatograms clearly show a sequential reduction in the peak for the starting material (Figure 26) as the mole ratio of chromium:fluorenone increases from 1:4 to 1:1, from an intensity of 6.00 to 1.00. However, there is not a concomitant rise in new product peaks, suggesting the reaction is forming large, insoluble molecules, possibly the unanalyzed carbonaceous material.

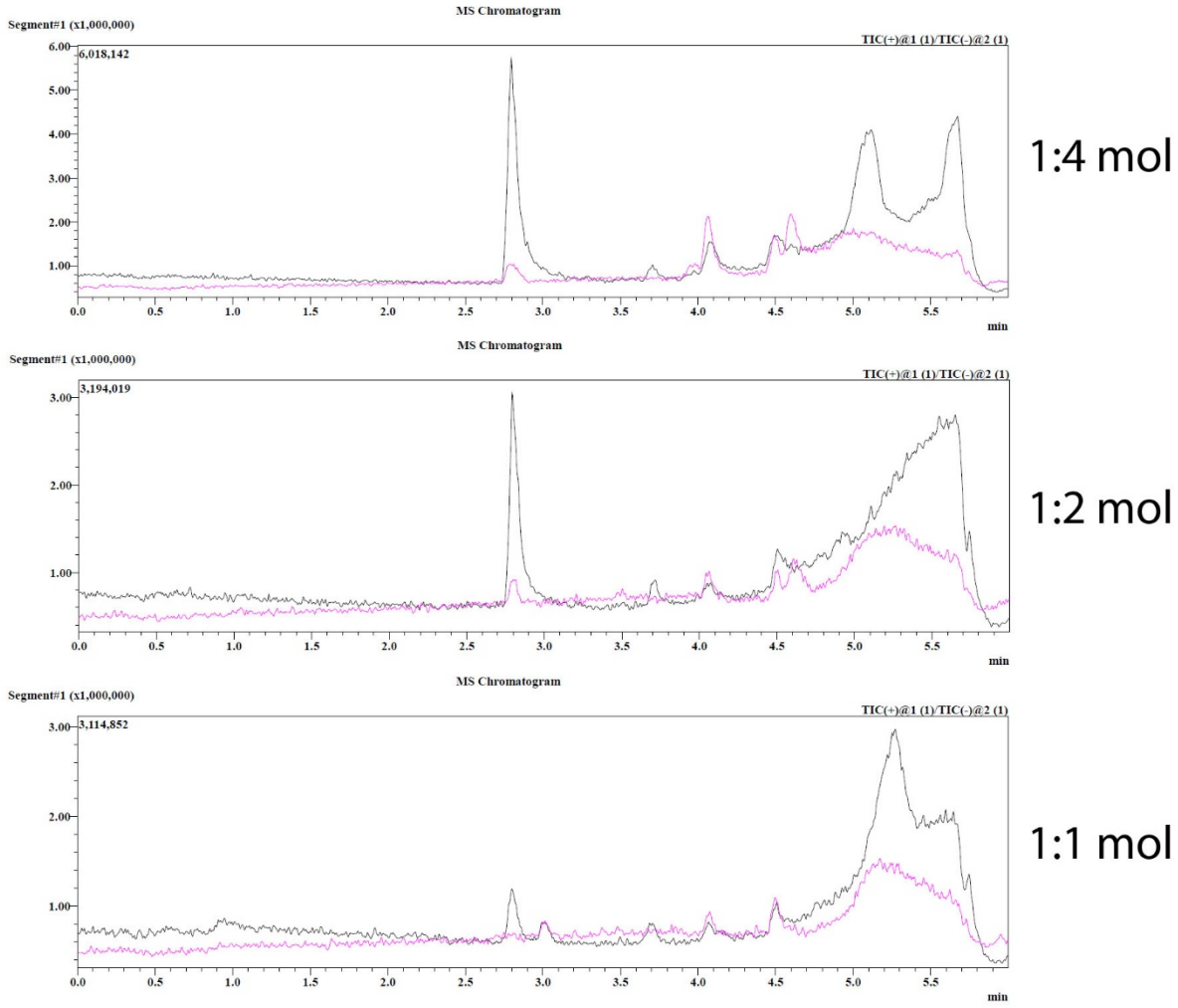

Figure 26. MS Chromatograms for trials with 9-fluorenone and chromium carbonyl by stoichiometric ratio.

Due to the difficulty in developing methods involving neat, molten reagents, benzophenone was selected for a survey of reaction conditions. The low melting point ensured liquid reaction mixtures, necessary due to poor stirring in the microwave instrument. Figure 27 show the LC-MS results of trials based on temperature and time. The control

reaction of unheated starting material indicates the position of benzophenone in the LC chromatogram. The heated trials show new peaks at elution times following this peak. Equilibrium seems to be reached in trials (d) and (f) whose chromatograms appear similar; these conditions were 130° C for 1 hr and a ramp to 170° C.

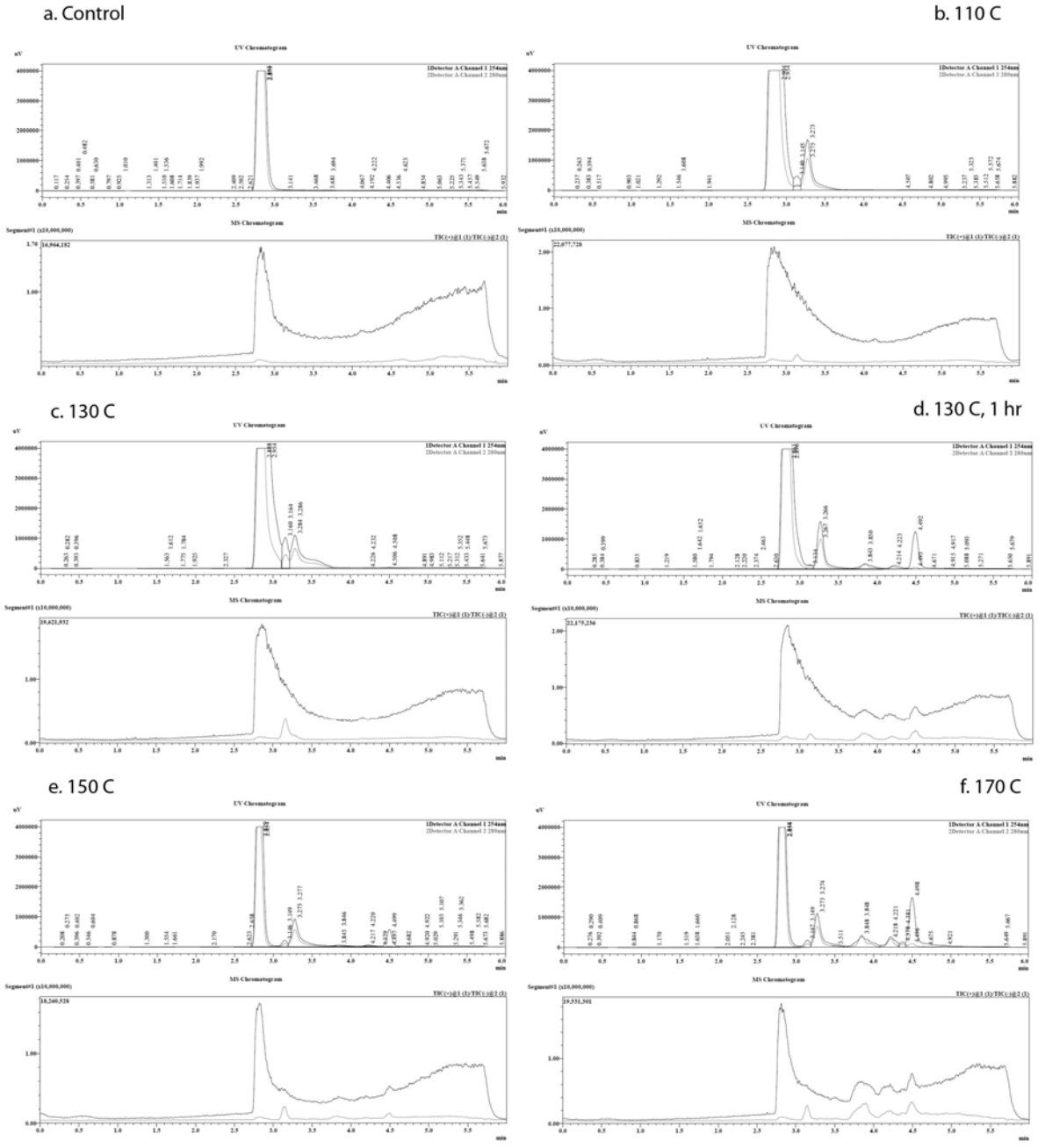

Figure 27. LC-MS spectra for benzophenone/cr(co)$_6$ trials by temperature and time. Control trial (a) was not heated. Trial (d) was heated for 1 hour at 130 C. The rest of the trials were heated until the reaction temperature reached the indicated set point.

These data show formation of new products at and above 130^0 C. The major absorption peak can be identified by MS as the starting material, but background mass peaks makes identification of the new peaks difficult. For example, in the MS spectrum for 170^0 C at elution time 4.5, in the negative ionization mode (event 2), there are three possible peaks of interest 249, 385 and 521 m/z. The major peak is 249, but it also appears as a major peak in all the negative mode spectra at different elution times. The 385 and 521 m/z peaks can be seen to grow in over time. It's not clear that any of the major peaks for this elution time can be assigned to the peak seen in the UV absorption spectrum. Furthermore, some UV peaks have no corresponding peak in the MS chromatogram, indicating at least some products are not ionizable by the instrument. Altogether, these results make the LC-MS data inadequate for assigning product identity.

Much more work needs to be done to understand this reaction system. Multiple modes of coupling appear to be occurring simultaneously. Unanswered questions include the role of initial carbonyl dissociation from the metal center and the role of the atmosphere the reaction is under. Can ancillary ligands be used to control either the mode of coupling or the stereochemistry of the products? Can the reaction be made catalytic in chromium with additives such as chlorosilanes as with the McMurry reaction? Can either metallopinacols or carbenes be isolated from the reaction mixture to suggest a mechanism for the reaction? Conclusion. New coupling reactions with metal carbonyls were reported. Substrates containing carbonyl functionalities, including anhydrides, produce various different coupling products. In some cases, such as fluorenone, the product is the McMurry coupling product.

REFERENCES

(1) Tsai, C.-C. *J. Chem. Educ.* **2001**, *78*, 970-974.

(2) Pfeiffer, H. C. *Proc. SPIE* **2010**, *7823*.

(3) Mann, C. *Technology Review* **2000,** 43-48.

(4) Bishop, D. *Bell Labs Tech. J.* **2005**, *10*, 23-28.

(5) Kish, L. B. *Phys. Lett. A* **2002**, *305*, 144-149.

(6) Nero, J. Del; de Souza, Fabricio M.; Capaz, Rodrigo B. *J. Comput.Theor. Nanosci. 2***010,** *7, 503-516*.

(7) Flood, A.; Stoddart, J.; Steuerman, D.; Heath, J. *Science.* **2004**, *306*, 2055-2056.

(8) Schnorr, J. M.; Swager, T. M. *Chem. Mater.* **2011**, *23*, 646-657.

(9) Heller, I.; Kong, J.; Williams, K. a; Dekker, C.; Lemay, S. G. *J. Am. Chem. Soc.* **2006**, *128*, 7353-7359.

(10) Komatsu, N.; Wang, F. *Materials.* **2010**, *3*, 3818-3844.

(11) Omachi, H.; Segawa, Y.; Itami, K. *Acc. Chem. Res.* **2012**, 1378–1389.

(12) Karousis, N.; Tagmatarchis, N.; Tasis, D. *Chem. Rev.* **2010**, *110*, 5366-5397.

(13) Dodziuk, H.; Hoffmann, R. *Strained hydrocarbons: beyond the van't Hoff and Le Bel hypothesis*; Wiley-VCH, 2009; pp. 354–355.

(14) Parekh, V. C.; Guha, P. C. *J. Indian Chem. Soc.* **1934**, 95.

(15) Friederich, R.; Nieger, M.; Vögtle, F. *Chem. Ber.* **1993**, 1723-1732.

(16) Segawa, Y.; Miyamoto, S.; Omachi, H.; Matsuura, S.; Šenel, P.; Sasamori, T.; Tokitoh, N.; Itami, K. *Angew. Chem. Int. Ed. Engl.* **2011**, *50*, 3244-3248.

(17) Jasti, R.; Bhattacharjee, J.; Neaton, J. B.; Bertozzi, C. R. *JACS Commun.* **2008**, 17646-17647.

(18) Takaba, H.; Omachi, H.; Yamamoto, Y.; Bouffard, J.; Itami, K. *Angew. Chem. Int. Ed. Engl.* **2009**, *48*, 6112.

(19) Yamago, S.; Watanabe, Y.; Iwamoto, T. *Angew. Chem. Int. Ed. Engl.* **2010**, *49*, 757.

(20) Fluorophore, O.; Sisto, T. J.; Golder, M. R.; Hirst, E. S.; Jasti, R. *J. Am. Chem. Soc.* **2011**, 15800.

(21) Xia, J.; Jasti, R. *Angew. Chem. Int. Ed. Engl.* **2012**, *51*, 2474.

(22) Sisto, T. J.; Tian, X.; Jasti, R. *J. Org. Chem.* **2012**, *77*, 5857.

(23) Darzi, E. R.; Sisto, T. J.; Jasti, R. *J. Org. Chem.* **2012**, *77*, 6624.

(24) Xia, J.; Bacon, J. W.; Jasti, R. *Chem. Sci.* **2012,** *3,* 3018-3021.

(25) Iwamoto, T.; Watanabe, Y.; Sakamoto, Y.; Suzuki, T.; Yamago, S. *J. Am. Chem. Soc.* **2011**, *133*, 8354.

(26) Iwamoto, T.; Watanabe, Y.; Sadahiro, T.; Haino, T.; Yamago, S. *Angew. Chem. Int. Ed. Engl.* **2011**, 8342.

(27) Kayahara, E.; Sakamoto, Y.; Suzuki, T.; Yamago, S. *Org. Lett.* **2012**, *14*, 3284.

(28) Segawa, Y.; Šenel, P.; Matsuura, S.; Omachi, H.; Itami, K. *Chem. Lett.* **2011**, *40*, 423.

(29) Jagadeesh, M. N.; Makur, A.; Chandrasekhar, J. *J. Mol. Model.* **2000**, *6*, 226.

(30) Wong, B. M. *J. Phys. Chem. C. Nanomater. Interfaces* **2009**, *113*, 21921.

(31) Sundholm, D.; Taubert, S.; Pichierri, F. *Phys. Chem. Chem. Phys.* **2010**, *12*, 2751.

(32) Segawa, Y.; Omachi, H.; Itami, K. *Org. Lett.* **2010**, *12*, 2262.

(33) Segawa, Y.; Fukazawa, A.; Matsuura, S.; Omachi, H.; Yamaguchi, S.; Irle, S.; Itami, K. *Org. Biomol. Chem.* **2012**, *10*, 5979.

(34) Lee, Y.; Choi, S.; Lee, S.; Chung, Y.; Kang, T. *Tetrahedron Lett.* **2006,** *47,* 6569–6572.

(35) Foster, Nancy; Forbes, M. *Technology Review* **2003**, 18-19.

(36) Kudinov, A. R.; Loginov, D. A.; Petrovskii, P. V. *Russ. Chem. Bullletin, Int. Ed.* **2007**, *56*, 1930.

(37) Cho, H. Y.; Ajaz, A.; Himali, D.; Waske, P. a; Johnson, R. P. *J. Org. Chem.* **2009**, *74*, 4137.

(38) McMurry, J. *Chem. Rev.* **1989**, *89*, 1513.

(39) Tyrlik, S.; Wolochowicz, I. *Bull. Soc. Chim. Fr.* **1973**, 2147.

(40) Mukaiyama, T.; Sato, T.; Hanna, J. *Chem. Lett.* **1973**, 1041.

(41) McMurry, J. E.; Fleming, M. P. *J. Am. Chem. Soc.* **1974**, *96*, 4708.

(42) Fuerstner, A.; Hupperts, A. *J. Am. Chem. Soc.* **1995**, *117*, 4468.

(43) Pierce, K.; Barteau, M. *J. Org. Chem.* **1995**, *60*, 2405.

(44) Villiers, C.; Ephritikhine, M. *Chem. Eur. J.* **2001**, *7*, 3043.

(45) Clive, D.; Murthy, K. *J. Am. Chem. Soc.* **1990**, *112*, 3018.

(46) McMurry, J.; Dushin, R. *J. Am. Chem. Soc.* **1990**, *112*, 6942.

(47) Nicolaou, K.; Yang, Z.; Liu, J.; Ueno, H. *Nature* **1994**, *367*, 630.

(48) Iyoda, M. *Pure Appl. Chem.* **2010**, *82*, 831.

(49) Kawase, T. *Synlett* **2007**, *2007*, 2609.

(50) Dubois, F.; Gingras, M. *Tetrahedron Lett.* **1998**, *39*, 5039.

(51) Komatsu, K.; Murata, M.; Murata, Y. *Science* **2005**, *307*, 238.

(52) Song, Y.; Di, C.-A.; Wei, Z.; Zhao, T.; Xu, W.; Liu, Y.; Zhang, D.; Zhu, D. *Chemistry* **2008**, *14*, 4731.

(53) Ter Wiel, M. K. J.; van Delden, R. a; Meetsma, A.; Feringa, B. L. *J. Am. Chem. Soc.* **2003**, *125*, 15076.

APPENDIX

Appendix A Experimental

Experimental. Cycloparaphenylene was synthesized following the procedures developed by Itami, et al. in various publications.[14-15]

Synthesis of cis-1,4-bis(4-bromophenyl)cyclohexane-1,4-diol, "L-unit". The L-unit was synthesized by the procedure described by Itami, et al. in their second published cpp synthesis.[14]

To a 500 mL round bottom flask were added lithium chloride (14.13 g, 327mmol) and cerium (III) trichloride heptahydrate (12.42 g, 31.7mmol). These were heated at 90 °C on an oil bath for 2 hrs under vacuum. The resulting hard, white solid was broken up with a spatula, pulverized with a mortar and pestle, and returned to the round bottom flask with an oven-dried stir bar. The mixture was again heated under vacuum at 90°C for 1 hr. Stirring was initiated and the temperature increased to 150 °C for 3 hrs. The round bottom flask was removed from heat, cooled, and pumped into a glovebox. Dry THF (~200 mL) was added and the resulting solution/suspension was stirred overnight.

The following day, to the 500 mL round bottom flask were added cyclohexane-1,4-dione (1.869 g, 15.8mmol). The resulting solution was stirred for an additional hour, then the flask was fitted with a plastic cap and rubber septum, and removed and cooled on a dry ice/acetone bath to -78 °C. Care was taken to ensure the solution didn't freeze or produce a suspension of crystallites. In addition, it was verified that vigorous stirring was achieved through the Dewar flask holding the bath.

In a glovebox, to a 500 mL round bottom flask were added a stir bar, 1,4-dibromobenzene (11.795 g, 47.7mmol) and dry THF (100 mL). The flask was fitted with a plastic cap and rubber septum, removed and cooled -78 °C. Care was taken to ensure the solution didn't freeze or produce a suspension of crystallites. In addition, it was verified that vigorous stirring was achieved through the Dewar flask holding the bath.

Once cooled, the n-butyl lithium (2.2 M in hexanes, 31 mL,49.6mmol) was added drop wise with vigorous stirring to the 1,4-bromobenzene. The solution was stirred for 30 minutes and then added drop wise to the salt suspension via cannula with vigorous stirring.

This final solution was stirred for ~1 hr at -78 °C and then left to stir overnight, reaching room temperature.

To work up, the solution was quenched with NH_4Cl, filtered over celite to remove solid salts, extracted with ethyl acetate, dried over Na_2SO_4, and concentrated under reduced pressure. The resulting white solid was recrystalized in chloroform. (2.59 g, 31.9% yield)

^{1}H NMR (300 MHz, $CDCl_3$) δ 1.71 (brs), 2.07 (s), 7.37 (d), 7.46 (d).

Synthesis of Methoxy Methyl Chloride. Methoxy methyl chloride was synthesized for protection of L-Unit.

To a 250 mL round bottom flask were added dimethoxy methane (54.0 mL, 610 mmol) and hexanoyl chloride (97.9 mL, 700 mmol). A stir bar was added and the flask was fitted with a reflux condenser. The reaction mixture was refluxed under nitrogen for 24 hours.

The condenser was removed and replaced with a still head. The reaction mixture was distilled. After discarding the first few drops, methoxy methyl chloride (36.38 g, 74.0%) was collected at approximately 55 °C.

^{1}H NMR (300 MHz, $CDCl_3$) δ 5.39 (s) and 3.44 (s).

MOM protection of L-unit. The protection of the L-unit was reproduced as described by Itami.[14]

To a 200 mL flat bottom flask were added cis-1,4-bis(4-bromophenyl)cyclohexane-1,4-diol (“L-unit”, 10.407 g, 24.4 mmol), diisopropylethylamine (18 mL, 103.3 mmol) 100 mL dry dichloromethane and a stir bar. The flask was fitted with a septum and cooled on an ice water bath with stirring for 15 minutes. Methoxymethyl chloride (9 mL, 118.5 mmol) was added through the septum, rapidly evolving gas. This reaction mixture was stirred for 18 hrs.

The resulting solution was quenched with NH_4Cl, extracted with DCM, dried over Na_2SO_4 and concentrated under reduced pressure. The resulting solid was separated on a silica gel column (DCM/hexanes), yielding the MOM protected L-unit (10.21 g, 82.2% yield.)

^{1}H NMR (300 MHz, $CDCl_3$) δ 2.01 (brs), 2.25-2.28 (brs), 3.39 (s), 4.41 (s), 7.31 (d), 7.44 (d).

Shotgun Macrocyclization of Mom-protected L-unit. The protected L-unit was cyclized following Itami's "shotgun" method.[15]

In a glove box, to a 250 mL round bottom flask were added $Ni(cod)_2$ (0.54 g, 1.96 mmol), 2,2'-dipyridyl (0.303 g, 1.95 mmol), mom-protected L-unit (0.56 g, 1.09 mmol) and dry THF (100 mL). Upon addition, these reagents produced a dark blue, almost black solution. The round bottom was fitted with a condenser and duck head. The duck head inlet was blocked with electrical tape. The assembled reaction vessel was removed from the glove box and quickly placed under nitrogen after removing the tape. Shortly after heating began, the solution turned a dark red color.

The reaction was stirred at reflux for 24 hrs. After cooling, the reaction mixture was filtered over celite, washed with ethyl acetate and chloroform, and concentrated under reduced pressure. The resulting solid was separated by silica gel chromatatron (hexanes/ethyl acetate) yielding the macrocyclic triangle, square and other cyclic oligomers.

Due the multiplicity of products and the difficulty of distinguishing them by NMR, no formal yield was calculated for this step. Itami recrystalizes after silica separation, but has only reported the tri- and tetramer. Through intense fractionation, I was able to isolate [15]- and [18]cpp, implying the pentamer and hexamer must also be produced at this step and that they must be virtually indistinguishable from the other oligomers by proton NMR.

^{1}H NMR (300 MHz, $CDCl_3$) δ 2.13 (brs), 2.36 (brs), 3.42 (s), 4.45 (s), 7.50 (m). (Tetramer.)

Variable Shotgun Macrocyclization. Once it had been determined that the macrocylcization was more dynamic than reported, attempts were made to incorporate additional structures into the macrocycles. For ease of setup, sealed Schlenk flasks were used instead of RBFs with reflux condensers under nitrogen.

In a glove box, to a 30 mL Schlenk flask were added $Ni(cod)_2$ (0.156 g, 566 μmol), 2,2'-bipyridine (0.097 g, 623 μmol), mom-protected L-unit (0.145 g, 282 μmol), p-dibromo

benzene (7.5 mg, 32 μmol) and dry THF (18 mL). The flask was sealed, removed from the glove box and stirred at 66 °C for 24 hrs.

After cooling, the reaction mixture was filtered over celite, washed with ethyl acetate and chloroform, and concentrated under reduced pressure. The resulting solid was separated by silica gel chromatatron (hexanes/ethyl acetate) yielding the macrocyclic oligomers. Other than general fractioning, no attempt was made to isolate different sizes. These fractions were carried forward to the final reduction/aromatization step.

Thermal Reduction of macrocycle to cycloparaphenylene.[15]

To a 125 mL test tube were added macrocyle (62 mg, 43.8 μmol), $NaHSO_4 \cdot H_2O$ (210 mg, 1.52 mmol), dry DMSO (9 mL, 105 mmol), dry *m*-xylene (9 mL, 98.6 mmol) and a stir bar. The reaction was heated at reflux (~150 °C) for 72 hrs. The reaction mixture was extracted with water and ethyl acetate (removing DMSO), filtered over celite, dried on Na_2SO_4. The remaining solvent was removed on a vacuum line and the solid was redisolved in DCM and filtered through a silica plug to remove yellow polymer. The crude product was then separated on silica gel chromatatron to yield cycloparaphenylene.

^{1}H NMR (300 MHz, $CDCl_3$) δ 7.61 (s). ([12]cycloparaphenylene).

Microwave Reduction of macrocycle to cycloparaphenylene.[15]

To a 10 mL microwave vial were added macrocycle (20 mg, 14.1 μmol), 0.1 M *aq*. tosyl alcohol (150 μL, 1.50 mmol), 3 mL *m*-xylene and a stir bar. The vial was sealed, loaded into the microwave and heated at 150 °C with 300 W for 30 minutes.

The resulting yellow solution/suspension was passed through a silica gel plug (to remove yellow solids) and dried on a vacuum line. NMR of this crude solid showed no cycloparaphenylene.

Synthesis of 1,2,5,6-tetrabromocyclooctane. This intermediate was synthesized for subsequent generation of 1,5-dibromocyclooctadiene.

In a glovebox, to a 100 mL round bottom flask wrapped in tin foil were added cyclooctadiene (25 mL, 204 mmol), a stir bar and 20 mL dry DCM. The flask was sealed with a plastic cap and rubber septum, removed from the glovebox and placed on an ice water

bath with stirring. Another foil-wrapped round bottom flask with septum was placed on another ice water bath to which bromine (24 mL, 471 mmol) was added. After allowing both vessels to cool to bath temperature, the bromine was added dropwise to the cyclooctadiene via cannula. This reaction mixture was stirred on ice bath for five hours.

The reaction was then quenched with aqueous ammonium chloride, extracted with DCM, dried over sodium sulfate, filtered and concentrated under reduced pressure, yielding an orange white solid. This crude was purified by recrystalization from DCM. The collected crystals were washed with DCM and dried on vacuum line. NMR analysis shows presence of both diastereomers, but primarily (1R,5R)-1,2,5,6-tetrabromocyclooctane (10:1 excess).

^{1}H NMR (300 MHz, $CDCl_3$) δ 4.76 (s), 2.79 (d), 2.13 (d). ((1R,5R)-1,2,5,6-tetrabromocyclooctane).

^{1}H NMR (300 MHz, $CDCl_3$) δ 4.56 (m), 2.51 (m), 2.43 (m). (1R,6S)-1,2,5,6-tetrabromocyclooctane.

*Synthesis of 1,5-dibromocyclooctadiene.*Dibromocyclooctadiene was produced as a potential structure of interest for addition in macrocyclization.

In a glovebox, to a 250 mL round bottom flask were added 1,2,5,6-tetrabromocyclooctane (4.015 g, 9.47 mmol), a stir bar and 30 mL dry THF. To a 100 mL round bottom flask were added potassium *t*-butoxide (2.2 g, 19.65 mmol) and 50 mL dry THF. These were sealed with a plastic cap and rubber septum, removed from the glovebox and cooled on dry ice/acetone baths to -78 °C. Once cooled, the potassium *t*-butoxide solution was added dropwise to the tetrabromocyclooctane via cannula with vigorous stirring. After addition, dry ice bath was replaced with ice water, allowing reaction mixture to warm to 0 °C. The reaction was stirred for an additional two hours at this temperature and then quenched with 200 mL petroleum ether and 500 mL water.

The reaction mixture was extracted with ethyl acetate, the organic phase washed with water, dried on sodium sulfate and concentrated under reduced pressure. This crude product mixture was separated by vacuum distillation. NMR analysis shows adequate separation of the 1,5- and 1,6- isomers and some cyclooctatetraene.

^{1}H NMR (300 MHz, $CDCl_3$) δ 6.09 (q), 2.81 (m), 2.42 (m). (1,5-dibromocyclooctadiene).

Synthesis of bis(benzene)chromium salt. The first half of the classic Fisher-Haffner synthesis was reproduced.[16]

In a glove box, to a 80 mL pressure flask were added aluminum powder (70 mg, 2.59 mmol), chromium trichloride (500 mg, 3.16 mmol) and benzene (25 mL, 269 mmol). The pressure flask was sealed and removed from glove box to an oil bath. The reaction mixture was heated at 150 for four days. The vessel was returned to glove box and the reaction mixture was filtered on a fine frit and washed with benzene.

This reaction failed to give crude product of the color described in the literature and so was abandoned after a few attempts.

Microwave Synthesis of Arene Chromium Carbonyls. A variety of arenes where metallated with chromium carbonyl for comparison with cycloparaphenylene.

In a glovebox, to a 10 mL microwave vial with stir bar were added chromium hexacarbonyl (111 mg, 504 μmol), terphenyl (71.0 mg, 308 μmol) or other arene, 3 mL dry THF and 3 mL di-*n*-butyl ether. The vial was capped, removed from the glovebox, and placed in a microwave reactor. The reaction mixture was heated for 1.5 hours at 150 °C with stirring. Upon completion, the vial was removed from the microwave and allowed to cool. Upon cooling, the bright yellow solution produced a large amount of yellow crystals. The solid was collected by filtration and purified by sublimation of the starting materials.

Synthesis of Bis(benzene)iron Salt. This was synthesized as a precursor for arene exchange.

In a glovebox, to a 250 mL round bottom flask with stir bar were added anhydrous iron trichloride (5.00 g, 30.8 mmol), anhydrous aluminum trichloride (12.3 g, 92.4 mmol) and dried and air-free benzene (100 mL, 1.12 mol). The flask was fitted with a condenser, removed from the glovebox, placed under nitrogen and heated at reflux overnight.

The reaction vessel was removed from heat, cooled on an ice bath and quenched with water. The mixture was extracted and the aqueous phase filtered and washed with hexanes.

This orange aqueous solution was added to aqueous ammonium hexafluorophosphate, precipitating an orange solid bis(benzene)iron·2[PF6] salt (7.43 g, 49.3%). The solid was dried on a vacuum line and NMR in acetonitrile showed salt with residual benzene. This solid was carried forward without further purification.

^{1}H NMR (300 MHz, CD_3CN) δ 6.96 (s).

Synthesis of (μ^5-cyclohexadienyl)(η^6-benzene)iron Hexafluorophosphate.

To a 100 mL round bottom flask were added bis(benzene)iron hexafluorophosphate salt (1.05 g, 2.09 mmol), sodium borohydride (85.0 mg, 2.25 mmol) and 10 mL THF. This solution was stirred for two hours and then the solvent was removed under reduced pressure. The resulting solid was dissolved in a minimum of DCM and precipitated by addition of diethyl ether. This solid was filtered and collected. Analysis by NMR in acetonitrile showed desired product.

^{1}H NMR (300 MHz, CD_3CN) δ 6.95 (m), 6.20 (s), 4.78 (m), 3.42 (m), 1.08 (d).

Solar Arene Exchange for Generation of (μ^5-cyclohexadienyl)(η^6-cycloparaphenylene)iron. A few initial attempts were made to exchange the iron complex onto cycloparaphenylene.

To a 20 mL vial were added (μ5-cyclohexadienyl)(ŋ6-benzene)iron hexafluorophosphate (2 mg, 6 μmol), [15]cycloparaphenylene (5 mg, 4 μmol), 1 mL DCM and 1 mL dibutyl ether. This mixture was capped and placed in a window with excellent afternoon sunlight exposure in a foil half-enclosure. In the afternoon, the DCM would reflux. This mixture was allowed to react for one week before analysis. Analysis was carried out by TLC and NMR and was inconclusive, no product compound was isolated.

Graphite Sensitized Generation of Fluorescent, Graphitic Particles. Reactions of this type were explored for possible application to the extension of cycloparaphenylene into carbon nanotubes.

To a small quartz test tube were added phthalic anhydride (1.87 g, mol) and graphite powder (100 mg). This test tube was placed in a small beaker which was then placed

in a 150 °C oven for ten minutes. This melted the phthalic anhydride allowing the graphite powder to form a suspension which quickly solidified at ambient temperature.

Into the quartz test tube was inserted a plug of glass wool. This quartz test tube was placed in a 10 mL microwave vial which was then capped, purged with nitrogen, and installed in the microwave reactor. The reaction was brought to 300 °C with 300 W and held there for one minute. The reaction was allowed to cool in the microwave.

The cooled vial was removed and the quartz test tube removed from it with tweezers. The side wall of the quartz test tube below the glass wool was thoroughly coated with a highly lustrous material. Removal of the glass wool showed brittle sheets of metallically shiny material were attached, apparently the same substance that coated the side walls. The interior of the test tube contained mostly amorphous, carbon black material.

The quartz test tube was extracted with hexane, DCM and ethyl acetate. This extract was filtered through silica/celite to remove graphite or other carbonaceous particles. The filtered extract was seen to fluoresce brightly by 366 nm excitation. The solvent was removed by reduced pressure and an NMR taken in chloroform, showing no signal, but still fluorescing brightly. An IR of the solid extract was taken as well.

Metal Carbonyl Coupling Reaction. In a glovebox, to a microwave vial were added 10.0 mmol of carbonyl containing substrate (e.g. 1.48 g phthalic anhydride) and 5.00 mmol metal carbonyl (e.g. 1.10 g chromium carbonyl). The microwave vial was then sealed with a cap, removed from the glove box and sealed in the microwave reactor. The vessel was heated under 200 W to 250 C. The vessel was allowed to cool.

For analysis the sample was dissolved in ~8 mL acetonitrile. A 0.5 mL aliquot was removed, passed through a microfilter into an LC-MS vial, then diluted 1:4 with acetonitrile. LC-MS was performed with a 6 min scan of 5-99 gradient water/formic acid.

Appendix B Comprehensive Data Table

Table 2. Comprehensive data table for [9]-, [12]-, and [15]cycloparaphenylene.

[x]cpp	Calculated HOMO (eV)[25]	Oxidation Potential (V)[25]	Absorption Max (nm)[25]	Fluorscence Max (nm)	^{1}H NMR (ppm)	^{13}C NMR (ppm)[25]	A_1 (cm^{-1})	E (cm^{-1})
9	-5.125	0.7	341	489	7.52	127.51, 138.02	1956	1872
12	-5.263	0.83	339	416	7.61	127.33, 138.49	1959	1878
15	-5.289			417	7.67	127.3, 138.8	1962	1888

Appendix C Crystal Structure of Spirobisanthracenedione

Crystal Data. 9,9'-spirobi[anthracene]-10,10'-dione is a new compound and its unit cell data and crystal structure are reported here.

Table 3. Unit cell data for 9,9'-spirobi[anthracene]-10,10'-dione.

Formula	$C_{27}H_{16}O_2$
Space Group	P-1
Cell Lengths (Å)	**a**=8.4453(5), **b**=8.9232(5), **c**=13.5764(7)
Cell Angles	**α**=96.190(2), **β**=93.793(2), **γ**=115.472(2)
Cell Volume ($Å^3$)	911.025
Z, Z'	Z=2, Z'=0
R-Factor (%)	4.24

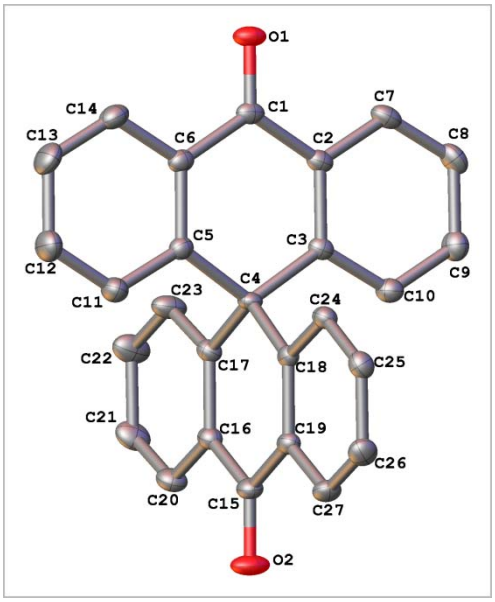

Figure 28. Crystal structure of 9,9'-spirobi[anthracene]-10,10'-dione.

Crystal Coordinates:

Label	X	Y	Z
O1	0.31556(8)	-0.13743(7)	0.03903(4)
O2	0.92734(9)	0.64840(8)	0.50800(5)
C1	0.40717(9)	-0.01987(9)	0.10492(5)
C2	0.56051(9)	-0.01877(9)	0.16456(5)
C3	0.66474(9)	0.11379(8)	0.24020(5)
C4	0.62517(9)	0.26352(8)	0.26876(5)
C5	0.46843(9)	0.25753(9)	0.20315(5)
C6	0.36563(9)	0.12398(9)	0.12823(5)
C7	0.60208(11)	-0.15411(9)	0.14309(6)
H7	0.5296	-0.2452	0.0925
C8	0.74729(11)	-0.15613(10)	0.19481(6)
H8	0.7751	-0.2479	0.1799
C9	0.85289(11)	-0.02238(10)	0.26917(6)
H9	0.954	-0.0224	0.3043
C10	0.81139(10)	0.11054(10)	0.29220(6)
H10	0.8832	0.2001	0.3437
C11	0.42420(11)	0.39106(10)	0.22091(6)
H11	0.4949	0.4839	0.2709
C12	0.27927(12)	0.39019(12)	0.16698(7)
H12	0.2506	0.4817	0.1803
C13	0.17480(12)	0.25517(12)	0.09288(7)
H13	0.0741	0.2536	0.0563
C14	0.21911(10)	0.12422(11)	0.07334(6)
H14	0.1496	0.0331	0.0221
C15	0.83895(10)	0.53632(9)	0.43899(5)
C16	0.67936(9)	0.38816(9)	0.45444(5)
C17	0.57835(9)	0.26086(9)	0.37582(5)
C18	0.78838(9)	0.42159(8)	0.25653(5)
C19	0.88820(9)	0.54643(9)	0.33646(5)
C20	0.62959(11)	0.37826(10)	0.55088(6)
H20	0.6994	0.4654	0.6041
C21	0.48068(12)	0.24361(11)	0.56927(6)
H21	0.4481	0.2372	0.6349
C22	0.37821(13)	0.11685(11)	0.49085(6)
H22	0.2747	0.0239	0.5028
C23	0.42673(11)	0.12587(10)	0.39540(6)

H23	0.3557	0.0388	0.3424
C24	0.84038(9)	0.44033(9)	0.16092(5)
H24	0.773	0.3564	0.1057
C25	0.98908(10)	0.58017(9)	0.14639(6)
H25	1.0227	0.5924	0.0812
C26	1.09010(10)	0.70350(10)	0.22712(6)
H26	1.1931	0.7988	0.2171
C27	1.03984(10)	0.68655(9)	0.32126(6)
H27	1.1085	0.7704	0.3762